Transfer RNA Maturation Defects Lead to Inhibition of ribosomal RNA Processing via Synthesis of pppGpp

Aude Trinquier, Jonathan E Ulmer, Laetitia Gilet, Sabine Figaro, Philippe Hammann, Lauriane Kuhn, Frédérique Braun, Ciaran Condon

Transfer RNA maturation defects lead to inhibition of ribosomal RNA processing via synthesis of pppGpp

Aude Trinquier, Jonathan E. Ulmer[1], Laetitia Gilet, Sabine Figaro, Philippe Hammann[2], Lauriane Kuhn[2], Frédérique Braun* and Ciarán Condon*

*Co-corresponding senior authors

UMR8261 (CNRS-Université Paris Diderot),

Institut de Biologie Physico-Chimique, 13 rue Pierre et Marie Curie, 75005 Paris, France

Lead contact : Ciarán Condon

[1]Current address : UMR3664, Institut Curie-PSL-CNRS, 26 rue d'Ulm, 75248 Paris Cedex 05, France

[2]Plateforme Proteomique Strasbourg – Esplanade, Institut de Biologie Moléculaire et Cellulaire, CNRS FR1589, 15 rue Descartes, 67084 Strasbourg cedex, France

Key words: tRNA; rRNA; ppGpp; stringent response; ribosome biogenesis; RNA maturation

Character count: 40,878

Correspondence:

Tel: (33)-1-58 41 51 23

Fax: (33)-1-58 41 50 20

E-mail: condon@ibpc.fr; frederique.braun@ibpc.fr

Summary

Ribosomal RNAs and transfer RNAs universally require processing from longer primary transcripts to become functional for translation. Here we describe an unsuspected link between tRNA maturation and the 3’ processing of 16S rRNA, a key step in preparing the small ribosomal subunit for interaction with the Shine-Dalgarno sequence in prokaryotic translation initiation. We show that an accumulation of either 5’ or 3’ immature tRNAs triggers RelA-dependent production of the stringent response alarmone (p)ppGpp in the Gram-positive model organism *Bacillus subtilis*. The accumulation of (p)ppGpp and accompanying decrease in GTP levels specifically inhibit 16S rRNA 3’ maturation. We suggest that cells can exploit this mechanism to sense potential slow-downs in tRNA maturation and adjust rRNA processing accordingly to maintain the appropriate functional balance between these two major components of the translation apparatus.

Introduction

Ribosomes are the platform for protein synthesis in all cells. Remarkably, the peptidyl transfer activity of this large ribonucleoprotein complex is provided by its RNA component, and the discovery of this property of ribosomes and those of other catalytic RNAs (ribozymes) has fueled the notion of an ancient RNA world in which all the major cellular functions, transcription, translation and replication were once RNA-based. Bacterial ribosomes contain three ribosomal RNAs (16S, 23S and 5S rRNA) that are generally transcribed as part of a large 30S precursor molecule and that assemble with >50 ribosomal proteins to form this translation center (Noller and Nomura, 1987). In *E. coli* and in most other bacteria studied, transcription, initial separation of the individual rRNAs and r-protein assembly all occur concomitantly, and require additional co-factors and quality control check points along the way to ensure the correct order of events and a stable functional ribosome at the end of this intricate process (Shajani et al., 2011).

By far the greatest proportion of a bacterial cell's biosynthetic capacity and energy consumption is devoted to ribosome biogenesis (Bremer and Dennis, 1996). Because of this energy cost, rRNA transcription is tightly regulated to match the growth rate afforded by the culture medium, a phenomenon known as metabolic control (Pao and Gallant, 1978; Stent and Brenner, 1961). One of the key effectors of this process is guanosine penta- or tetra-phosphate, collectively referred to as (p)ppGpp, and historically known as magic spot (Cashel and Rudd, 1987). In *E. coli,* (p)ppGpp binds to RNA polymerase with the help of the DksA protein to down-regulate initiation at rRNA promoters at slower growth rates, or during amino acid starvation (the stringent response) when rRNA transcription is essentially halted (Ross et al., 2016). The stringent response permits a global readjustment of the cell’s metabolism, including inhibition of fatty acid biosynthesis, DNA replication, induction of amino acid biosynthesis and in the establishment of the persister cell state upon exposure to antibiotics or other severe stress conditions (Amato et al., 2013; Chowdhury et al., 2016; My et al., 2015; Polakis et al., 1973; Traxler et al., 2008; Wang et al., 2007). (p)ppGpp has also been implicated in the inhibition of translation by blocking the activity of translation factors EF-Tu, EF-G and IF2, and the association of ribosomal subunits through its interaction with ObgE (Feng et al., 2014; Miller et al., 1973; Milon et al., 2006; Mitkevich et al., 2010). In *B. subtilis,* (p)ppGpp is similarly an effector of the stringent response, but rather than binding to RNA polymerase, it inhibits the

synthesis of GTP by binding to two enzymes of the *de novo* and salvage pathways of GTP synthesis, Gmk and HprT, respectively (Kriel et al., 2012; Liu et al., 2015). Since ribosomal RNA promoters in both *E. coli* and *B. subtilis* are exquisitely sensitive to the concentration of the initiating nucleotide (iNTP), the decrease in GTP pools (the iNTP of all 10 rRNA operons in *B. subtilis*) leads to strong inhibition of rRNA transcription (Gaal et al., 1997; Krasny and Gourse, 2004).

The maturation of rRNA is also remarkably different between *E. coli* and *B. subtilis*, with only two processing reactions being shared out of at least ten known intermediary and final processing steps. The first is the co-transcriptional cleavage of the primary transcript by RNase III that occurs in the long double-stranded processing stalks formed by hybridization of complementary precursor sequences at the 5' and 3' ends of both 16S (Fig. 1A) and 23S rRNA. Cleavage by RNase III separates the three rRNA molecules, which subsequently undergo further processing reactions to yield the mature functional rRNAs (Dunn and Studier, 1973; Herskovitz and Bechhofer, 2000). The enzymes responsible for most of the final maturation steps in *E. coli*, RNase E, RNase G and RNase T, are not found in *B. subtilis* and *vice versa*, where the enzymes RNase J1, Mini-III and RNase M5 play the key roles (Condon, 2014). The only exception is the enzyme involved in the maturation of the 3’ end 16S rRNA, called YbeY in *E. coli* (Jacob et al., 2013) and YqfG in *B. subilis* (Baumgardt et al., 2018).

The final rRNA trimming steps serve to protect rRNAs from degradation by limiting access to exoribonucleases and are thought to occur at the end of the assembly of each subunit to rubber stamp the assembly process (Baumgardt et al., 2018; Li et al., 1998). Thus mutations that perturb 30S or 50S subunit assembly generally block the final processing of 16S and 23S rRNA (Bylund et al., 1998; Charollais et al., 2003; Hase et al., 2009; Hwang and Inouye, 2006; Nord et al., 2009; Sayed et al., 1999). In *E. coli* a number of maturation factors, including GTPases (RsgA, Era), RNA chaperones (RimM, RimP, RbfA) and modification enzymes (RimJ, KsgA etc.) are known to be involved in 30S ribosomal subunit assembly (Shajani et al., 2011). In addition to having homologs for each of these factors, *B. subtilis* has at least one additional GTPase, called YqeH, involved in the 30S assembly process (Loh et al., 2007; Uicker et al., 2007).

In this paper, we describe the discovery of a link between transfer RNA (tRNA) maturation by RNase P and RNase Z in *B. subtilis*, and processing of the 3’ end of 16S rRNA by

YqfG. RNase P is historically one of the first enzymes whose catalytic moiety was shown to be an RNA, encoded by the *rnpB* gene (Guerrier-Takada et al., 1983). Its primary function is the maturation of the 5' end of tRNAs. The enzyme also contains a small basic protein subunit, encoded by the *rnpA* gene, that plays a role in substrate recognition and binding (Crary et al., 1998; Reich et al., 1988). Although the RNA component of RNase P is sufficient for catalysis *in vitro*, both the RNA and protein moieties are essential for cell viability *in vivo* (Waugh and Pace, 1990; Wegscheid et al., 2006). There are two major pathways for the maturation of the 3' end of tRNAs in *B. subtilis*. About two-thirds of *B. subtilis* tRNAs (59 tRNAs whose CCA motif is encoded by their genes) are matured by a 3'-5 exoribonucleolytic pathway involving the redundant activities of RNase PH, PNPase, RNase R and YhaM (Wen et al., 2005). RNase Z is required for the 3' maturation of 17 *B. subtilis* tRNAs lacking a CCA motif encoded in their genes (Pellegrini et al., 2012; Pellegrini et al., 2003), while 10 non-CCA encoding tRNAs can be matured by either pathway (Wen et al., 2005). Here, we propose a model that couples tRNA maturation by RNases P and Z to 16S 3' maturation *via* the production of (p)ppGpp, a decrease in GTP levels and a defect in 30S ribosomal subunit assembly by GTPases.

Results

RNase P depletion inhibits maturation of the 3' end of 16S rRNA

In an experiment originally designed to identify enzymes involved in the maturation of 16S rRNA in *B. subtilis*, we screened a number of mutant strains lacking known ribonucleases for defects in 16S rRNA 3' processing, by Northern blotting of total RNA. In wild-type (wt) cells, a probe specific for 16S rRNA 3' precursors detects both full-length precursors (~1620 nts) and a 65-nt species extending from the proposed YqfG cleavage site to the downstream RNase III site (Fig. 1A) (Baumgardt et al., 2018 ; DiChiara et al., 2016). To our surprise, depletion of either the protein (*rnpA*) or RNA (*rnpB*) subunit of the tRNA 5' processing enzyme RNase P resulted in a strong reduction in 16S rRNA 3' processing as indicated by the absence of the 65-nt species (Fig. 1B). Depletion was achieved using integrative vectors that placed the native copy of the *rnpA* and *rnpB* genes under control of the xylose-inducible *Pxyl* promoter or the IPTG-inducible *Pspac* promoter, respectively, and growing cells in the presence of glucose to shut off expression of the *Pxyl-rnpA* construct or in the absence of IPTG to shut off expression of *Pspac-rnpB*.

Processing efficiency, quantified as the ratio of the 65-nt species to that of the full-length 16S rRNA precursor (65-nt/pre-16S), was reduced by 6.2 and 5.8-fold under conditions of *rnpB* and *rnpA* depletion, respectively, compared to those in the presence of inducer. Since we had already identified a candidate for the 16S rRNA 3' cleavage reaction, the essential enzyme YqfG (Baumgardt et al., 2018), we suspected the effect of RNase P depletion on 16S rRNA processing was indirect and was the consequence of a defect in tRNA maturation. Depletion of the RNA subunit of RNase P had a stronger effect on tRNA maturation than depletion of the protein subunit (Fig. S1), presumably reflecting the relative stabilities of the two components of the enzyme, and this more than likely accounts for the stronger effect of *rnpB* depletion on 3' processing of 16S rRNA.

The effect of RNase P depletion is specific for 3' end of 16S rRNA

We asked whether the effect of RNase P depletion was specific to the 3’ end of 16S rRNA or whether other rRNA processing reactions were affected. The 5’ end of 16S rRNA is matured by the 5’-exoribonuclease RNase J1 in *B. subtilis* (Britton et al., 2007; Mathy et al., 2007), while the 5' and 3' ends of 23S rRNA are simultaneously processed by the double-strand specific enzyme Mini-RNase III (Fig. S2A, B) (Redko et al., 2008). We examined the 5' processing of 16S and 23S rRNA by primer extension using an oligonucleotide complementary to the early mature sequences to detect 5' precursors extending as far as the upstream RNase III cleavage sites. By proxy, assay of 23S rRNA 5’ processing also determines the efficiency of 3’ processing, since both strands of the processing stalk are cleaved together (Redko et al., 2008). Depletion of *rnpA* did not have a major effect on 5' maturation of either 16S or 23S rRNA (Fig. S2C, D), indicating that the coupling with tRNA maturation is specific to the 16S rRNA 3' processing reaction.

Depletion of RNase Z has a similar effect on 16S 3' processing to depletion of RNase P

We next asked whether the inhibition of 16S 3' processing was restricted to RNase P or whether it would similarly occur in cells depleted for the tRNA 3' processing enzyme RNase Z, involved in the maturation of about one-third of *B. subtilis* tRNAs (Wen et al., 2005). In cells depleted for RNase Z, under the control of the *Pspac* promoter, the levels of the 65-nt species were strongly reduced, but not completely absent. This corresponded to a 2.2-fold decrease in

processing efficiency (Fig. 1C). Thus, while the effect of RNase Z depletion on 16S 3' processing is less severe than depletion of RNase P, presumably because it has fewer tRNA substrates than RNase P, it is nonetheless evident. This result suggests that the 16S rRNA 3’ processing defect is the result of a general deficiency in tRNA maturation.

3' processing of 16S rRNA is affected in mutants of the 30S subunit assembly pathway

The effect of the tRNA maturation defects on 16S rRNA processing could occur through an effect on the expression or activity of the 3' processing enzyme itself, YqfG, or on any of the major 30S ribosomal subunit assembly factors, since final processing is considered to occur post-assembly. We first screened a number of mutants lacking or depleted for specific 30S ribosomal proteins and assembly factors to determine which, if any, were affected in 16S rRNA 3' processing in *B. subtilis*. No major defects were observed in cells lacking the r-protein S5 acetylase RimJ orthologs YdaF or YjcK, the 16S rRNA methylase KsgA, the RNA chaperones RimP (YlxS in *B. subtilis*) or RbfA, or the r-protein S21 *(*Δ*rpsU*) (Fig. 2A, B). However, strains lacking the RNA chaperone RimM, the GTPases CpgA (equivalent to *E. coli* RsgA) or the *B. subtilis*-specific YqeH, all showed greater degrees of 16S rRNA 3' processing deficiency, as did cells depleted for the essential GTPase Era or the 3’ processing enzyme YqfG, as seen previously (Baumgardt et al., 2018). Thus, as in *E. coli*, a number of different proteins involved in *B. subtilis* 30S subunit biogenesis have an impact on 16S rRNA processing and are potential intermediates in the mechanism coupling 16S rRNA 3’ processing to tRNA maturation.

Depletion of RNase P or RNase Z results in altered mRNA levels of several key 30S assembly factors

We performed Northern blots to determine whether the expression of any of the genes encoding different 30S assembly factors with a major impact on 16S rRNA 3’ processing was altered in cells depleted for RNase P or RNase Z. Remarkably, mRNA levels coding for two 30S assembly proteins, the GTPases Era and YqeH, increased under depletion conditions for either tRNA maturase (Fig. 2C), while the expression of two mRNAs, encoding the RNA chaperone RimM and the GTPase CpgA, decreased (Fig. 2D). Some mRNAs were relatively unchanged (e.g. *rimP/ylxS*, *rbfA*), while others (e.g. *yqfG*) were too low to be detected by Northern blot (data not shown). Thus, under conditions of RNase P or Z depletion, the transcript levels of a number

of key assembly factors are perturbed and could account for the 16S 3' processing defect because their levels are insufficient for 30S assembly, or because they poison the assembly process when over-expressed.

Depletion of RNase P or RNase Z results in a defect in 30S subunit assembly

To determine whether a decrease in tRNA maturation levels leads to a defect in 30S subunit assembly in *B. subtilis*, we subjected ribosomes isolated from cells depleted for RNase P (*rnpA*) or RNase Z to sucrose gradient analysis under low magnesium (Mg) conditions (3 mM) to dissociate ribosomal subunits. Under RNase P and RNase Z depletion conditions, the 30S peak was slightly broader than that seen in wt cells, with a small shoulder corresponding to the early 30S fractions (Fig. 3A). The 16S ribosomal RNA present in these early fractions (fraction 10) is aberrant and shows two additional species, one slightly larger and one slightly smaller than mature 16S rRNA, corresponding to precursor and partially degraded 16S rRNA species (Fig. 3B). We have seen this pattern previously with the depletion of the 16S 3' processing enzyme YqfG (Baumgardt et al., 2018). We measured the levels of individual ribosomal proteins present in fraction 10 by mass spectrometry (LC-MS/MS) and compared them to the content of the mature 30S peak (fraction 12) of wt cells. In cells depleted for RNase P (*rnpA*), a number of late assembly ribosomal proteins were significantly reduced, including S2, S3, S14 and S21, which were present at ≤10% of wt, and S5, S9 and S13 which were ≤50% of wt (Fig. 3C). A milder but overlapping defect was observed with the RNase Z depletion strain, with the late proteins S2, S3 and S14 showing defective levels at ≤50% of wt (Fig. 3D). Thus, depletion of RNase P and RNase Z indeed results in a late 30S subunit assembly defect that could account for the defect in 16S rRNA 3' processing. The observation that only specific (late) r-proteins were affected in this experiment confirms that at this point in the depletion curve, we have not yet reached the point of a global shut-down in r-protein synthesis.

The late assembly defect is very reminiscent of that seen in *E. coli* cells lacking RimM (Bunner et al., 2010; Guo et al., 2013; Leong et al., 2013), which along with *cpgA* was one of the two assembly factor mRNAs down-regulated by depletion of the tRNA maturation enzymes in *B. subtilis* (Fig. 2D). We therefore asked whether RimM performed a similar function in *B. subtilis* by performing sucrose gradient and mass spectrometry analysis similar to those described for the depletion of RNase P and RNase Z. In the Δ*rimM* strain, the 30S peak was shifted significantly

towards a precursor form (Fig. S3A), confirmed by the analysis of 16S rRNA, which showed primarily the precursor and degraded 16S rRNA species, and very little mature 16S rRNA (Fig. S3B). We analysed the r-protein content of fractions 10 and 11 from this gradient by mass-spectrometry and saw very similar defects to those observed with the RNase P and the milder RNase Z depletion strains, respectively. Fraction 10 showed reduced levels of the late assembly proteins S2, S3, S9, S10, S14, S19, S21 (≤50% of wt; Fig. S3C), whereas fraction 11 showed a milder defect with lower levels of S2, S3 and S14 (Fig. S3D). Thus, reduced levels of *rimM* expression in RNase P or RNase Z depletion strains could potentially account for the defect observed in 30S subunit assembly. In *E. coli,* RbgA (CpgA in *B. subtilis*) has been shown to have a similar role to RimM in late 30S assembly (Leong et al., 2013). Therefore, we also considered the possibility that the reduced *cpgA* mRNA levels in tRNA maturase depletion strains might equally contribute to the 30S assembly defect.

Perturbation of assembly factor mRNA levels upon RNase P depletion is not sufficient to account for the 16S rRNA processing defect.

To directly test the hypothesis that the decreased *rimM* and *cpgA* mRNA levels could account for the defect in 16S rRNA 3' maturation in strains depleted for tRNA processing enzymes, we asked whether we could complement the processing deficiency by ectopic expression of these two mRNAs. We constructed a single integrative vector expressing both *rimM* under control of the arabinose-dependent *Pxsa* promoter (Franco et al., 2007) and *cpgA* under control of the bacitracin-dependent *Plia* promoter (Toymentseva et al., 2012). Even leaky expression of *rimM* or *cpgA* from this construct was sufficient to complement the respective 16S 3' processing defects in *rimM* and *cpgA* mutants, showing that the construct is functional (Fig. S4A, compare lanes 3 and 4, and lanes 6 and 8). However, ectopic expression of *rimM* alone, or *rimM* with *cpgA,* failed to rescue the 16S rRNA 3' processing defect in cells depleted for *rnpB* (Fig. S4B, compare lane 6 and 4). Similarly, ectopic expression of the 3' processing enzyme YqfG (Baumgardt et al., 2018), whose native mRNA we had failed to detect by Northern blot (above), did not restore 16S rRNA 3' processing under RNase P depletion conditions (Fig. S4C). Lastly, overexpression of the GTPase genes *era* or *yqeH* from a plasmid in a wt background had no impact on 16S rRNA 3' maturation (Fig. S4D, E), ruling out the possibility that the increase in expression of these mRNAs observed in RNase P and RNase Z depletion strains could poison

30S subunit assembly. Although we haven't formally ruled out the possibility that multiple cumulative effects are responsible, these experiments suggest that the impact of tRNA processing defects on 16S rRNA 3' maturation is unlikely to be due to the perturbation of the expression of 30S assembly factors or processing enzymes alone.

Defects in tRNA processing lead to the induction of the stringent response *via* RelA

Having discounted the possibility that altered expression levels of 30S assembly factors were solely responsible for the 16S rRNA processing defect, we speculated that the activity of these proteins might be impacted by perturbations in tRNA processing. It was recently shown that the alarmone (p)ppGpp was a competitive inhibitor of GTPases involved in 30S ribosome biogenesis in *S. aureus*, notably Era and RbgA (CpgA in *B. subtilis*) (Corrigan et al., 2016). We therefore considered the possibility that the synthesis of (p)ppGpp might be induced by immature tRNA in a manner similar to the mechanism involving RelA and uncharged tRNA, *i.e. via* the stringent response. We first asked whether depletion of RNase P or RNase Z led to an accumulation of (p)ppGpp in *B. subtilis* by adding ^{32}P-labelled inorganic phosphate to cultures, extracting total nucleotides with formic acid and analyzing them by thin-layer chromatography (TLC). The migration position of (p)ppGpp was determined by adding the stringent response inducer arginine hydroxamate (RHX) to wt cells and to a ppGpp^0 strain unable to synthesize (p)ppGpp because it lacks the three known synthetases RelA, YwaC and YjbM (Kriel et al., 2012). Strains depleted for RNase P (*rnpA* or *rnpB*) showed strongly increased synthesis of pppGpp, while depletion of RNase Z showed a much weaker effect (Fig. 4A), coherent with their relative impacts on 16S 3' processing and 30S ribosome assembly. That the main form of the alarmone synthesized was the penta-phosphate derivative (pppGpp) was previously observed for *B. subtilis* (Wendrich and Marahiel, 1997).

Given the high back-ground signal in the TLC assay, we wished to confirm that the levels of (p)ppGpp observed upon depletion of RNase P or RNase Z were physiologically relevant. To do this, we assayed the expression of the *ywaA* and *ilvA* genes, two members of the *B. subtilis* CodY regulon, whose expression is known to increase during the stringent response due to resulting decrease in GTP pools (Kriel et al., 2012). The expression of both *ywaA* and *ilvA* was strongly derepressed in strains depleted for either the RNA or protein subunits of RNase P, and more weakly derepressed in response to depletion for RNase Z (Fig. 4B), consistent with the

direct assay of (p)ppGpp levels in these strains (Fig. 4A). We will use derepression of *ywaA* as an indirect measure of *in vivo* guanosine nucleotide pools for the rest of this paper.

To ask whether the synthesis of (p)ppGpp was dependent on the two synthetases YwaC and YjbM, or on the synthetase/hydrolase RelA, we examined the expression of *ywaA* in cells depleted for RNase P (*rnpA*) in a *ywaC yjbM* background or a strain lacking all three (p)ppGpp synthesizing enzymes. The experiment was done in this way because *relA* single mutants rapidly accumulate suppressor mutations in the two synthetase genes (Natori et al., 2009). Expression of *ywaA* was still strongly derepressed in the double *ywaC yjbM* mutant but no longer occurred in the triple *ywaC yjbM relA* mutant (ppGpp^0 strain; Fig. 4C), showing that the primary sensor of the tRNA maturation defect is the stringent response effector RelA.

16S 3' processing is partially restored in ppGpp^0 strains depleted for RNase P and RNase Z

If (p)ppGpp is an effector in the tRNA/16S rRNA maturation coupling mechanism, we would predict that 16S 3' processing should be impacted to a lesser degree by depletion of RNase P and RNase Z in ppGpp^0 strains. This was indeed the case. In RNase P depletion strains, 16S processing efficiency was partially restored in the ppGpp^0 background (Fig. 5). The processing efficiency improved from a 5.8-fold deficiency to only a 2.6-fold defect upon depletion of *rnpA* in a ppGpp$^+$ *vs*. ppGpp^0 background, and from 6.2-fold to 2.4-fold deficiency upon depletion of *rnpB*. In RNase Z depletion strains, which still show some 16S 3' processing in ppGpp$^+$ strains, there was no improvement in maturation efficiency the ppGpp^0 background (2.2-fold defect compared to 2.6-fold in ppGpp$^+$ *vs*. ppGpp^0 backgrounds; data not shown), consistent with the lower level of (p)ppGpp synthesis upon depletion of RNase Z and the generally milder effect of RNase Z depletion on 16S rRNA 3' processing. Since 16S rRNA maturation efficiency is not completely restored in a ppGpp^0 background, this suggests that (p)ppGpp is not the only effector of the coupling mechanism between tRNA and 16S rRNA 3' processing.

Increased (p)ppGpp levels and decreased GTP pools inhibit 16S 3' processing in the absence of tRNA processing defects

We next asked whether the synthesis of (p)ppGpp or a decrease in intracellular GTP levels would inhibit 16S rRNA 3' processing in the absence of a defect in tRNA maturation. We did this in three ways, each time using the CodY-regulated *ywaA* gene as a sensitive gauge of the

changes in nucleotide pools. We first asked whether classical induction of the stringent response by amino acid starvation would also lead to a defect in 16S 3' rRNA processing. Addition of RHX to wt cells led to a decrease in the production of the 65-nt species over time that significantly out-paced the rate of inhibition of 16S rRNA transcription, as measured by levels of remaining full-length precursor (Fig. 6A). Thus, induction of the stringent response not only inhibits rRNA transcription as previously observed, but also impedes 16S rRNA 3' processing. Second, we constructed a strain that allowed us to induce (p)ppGpp synthesis in the absence of either defects in tRNA processing or amino acid starvation. In this strain, the three (p)ppGpp synthetase genes (*ywaC, yjbM, relA*) were inactivated in their native loci and an ectopic copy of the *ywaC* synthetase gene was placed under control of the *Pxyl* promoter in the *amyE* locus. Addition of xylose to this strain led to a strong induction of ppGpp synthesis as measured by TLC (Fig. 6B) and this was confirmed by showing derepression of *ywaA* gene expression by Northern blot at different times after addition of xylose to the growth medium (Fig. 6C). Reduced levels of the 65-nt 16S 3' rRNA processed species were observed only 2 minutes after addition to xylose to the culture, well before synthesis of the full-length 16S rRNA precursor began to decrease, 15 minutes after xylose addition. In agreement, calculation of the processing efficiency (65-nt/full-length), showed a steady decrease over the full time-course of the experiment, even after the point where inhibition of 16S rRNA transcription became evident (Fig. 6C). Thus, induction of (p)ppGpp synthesis in the absence of amino acid starvation also results in a deficiency in 16S 3' processing. Lastly, we investigated whether a decrease in GTP synthesis would have an impact on 16S 3' rRNA processing independently of (p)ppGpp production, by adding the fungal GMP synthetase inhibitor decoyinine to cultures. Addition of decoyinine to wt cells led to a rapid decrease in 16S rRNA 3' processing efficiency, suggesting that a decrease in GTP levels is sufficient to inhibit the different GTPases that play a role in 30S ribosomal subunit assembly and ultimately cause the 16S rRNA 3' maturation defect (Fig. 6D). However, it does not rule out an additional contribution from direct inhibition of the ribosome biogenesis GTPases by (p)ppGpp, as proposed in *S. aureus* (Corrigan et al., 2016).

Discussion

This paper describes an intriguing observation that tRNA processing mutants completely abolish 16S 3' processing. We worked backwards from an original hypothesis that the expression

or activity of certain 30S ribosome assembly factors was affected to show that there was indeed a specific late 30S biogenesis defect. Finally, we discovered the missing link: that unprocessed tRNAs can induce the stringent response and the synthesis of (p)ppGpp. We propose a model in which unprocessed tRNAs enter the ribosome A-site similar to uncharged tRNA and trigger RelA-dependent (p)ppGpp synthesis (Fig. 7). The synthesis of (p)ppGpp can have two effects, either through direct competitive inhibition of assembly factor GTPase activity as proposed by Grundling and coworkers in *S. aureus* (Corrigan et al., 2016), or indirectly through the decrease in GTP pools necessary for their activity. Our data suggest that in *B. subtilis* at least, the decrease in GTP pools is sufficient to lead to problems in late 30S ribosome assembly and, consequently, to the deficiency in the maturation of 16S rRNA.

With only minor accommodations, the structure of RelA on the ribosome (PDB 5iqr) could accept both 5' and 3' tRNA precursors (Fig. S5). RelA recognizes C74 and C75 of the CCA motif of uncharged tRNA through a stacking interaction with His432 and hydrogen bond interactions with Arg438 (Arenz et al., 2016; Brown et al., 2016; Loveland et al., 2016). It is possible that similar interactions could occur with non-cytosine bases in the equivalent positions of non-CCA containing tRNA 3' precursors that accumulate in RNase Z-depleted cells. Since a free 3'-hydroxyl group of the terminal A-residue was proposed to be necessary for (p)ppGpp synthesis by RelA *in vitro* (Sprinzl and Richter, 1976), a different accommodation process would be necessary to account for the ability of 3' extended tRNA precursors to stimulate (p)ppGpp synthesis in RNase Z-depleted cells. It will be interesting to determine the molecular details of this recognition mechanism. Shetty and Varshney recently showed that three consecutive GC base pairs in acceptor stem of the initiator tRNA played an important role in licensing the final rRNA processing reactions during the first round of initiation complex formation in *E. coli* (Shetty and Varshney, 2016). Although these experiments did not directly implicate the stringent response, they showed that correct tRNA structure in the A-site is important for 16S rRNA processing. From a physiological standpoint, both these observations and ours indicate that other tRNA forms besides uncharged tRNA in the A-site may be able to activate RelA.

We have previously shown that the 16S 3' processing step is a quality control event that rubber stamps the correct completion of the 30S assembly process and that small subunits that are not processed correctly are rapidly degraded by RNase R (Baumgardt et al., 2018). Here, we show that inhibition of 16S 3' processing during the stringent response is much more rapid than

the inhibition of rRNA transcription. Hence, upon encountering translational stress, bacterial cells possess a mechanism not only to shut down transcription of rRNAs, but also to block the assembly of existing precursors into functional ribosomal subunits and to rapidly degrade the partially assembled pre-rRNAs. This suggests that the effect of (p)ppGpp production on *de novo* ribosome production is more rapid and extensive than previously understood. Our experiments show that cells can exploit this mechanism to sense potential slow-downs in tRNA maturation and adjust ribosome production accordingly. This would maintain the appropriate functional balance between these two major components of the translation apparatus. Indeed, it makes physiological sense to slow down ribosome assembly and processing under conditions where the levels of mature tRNAs available for translation are even transiently diminished. Expression levels of the *rnpA*, *rnpB* and *rnz* RNAs are relatively constant over about a hundred growth conditions tested (Nicolas et al., 2012), suggesting that the synthesis levels of these enzymes does not vary much in cells. We suspect therefore that the coupling mechanism may play a role in fine-tuning ribosome biogenesis and rRNA processing to minor perturbations in tRNA maturation that occur when the tRNA processing enzymes are transiently out-titrated by tRNA synthesis levels during the cell cycle.

Processing of the 3' end of 16S rRNA is restored to about half of its normal levels when tRNA maturation enzymes are depleted in a $ppGpp^0$ background, suggesting that (p)ppGpp is not the only effector of this coupling phenomenon. One possibility is that the perturbation in mRNA levels of the 30S assembly factors, in particular the decrease in levels of the mRNA encoding the GTPase CpgA contributes to this phenomenon. Although ectopic expression of *cpgA* failed to complement the 16S rRNA processing defect in cells depleted for RNase P, the ectopically produced enzyme would also be predicted to be inhibited by the ambient levels of (p)ppGpp and GTP in cells accumulating tRNA precursors. Second, although ectopic expression of the RNA chaperone RimM or the 16S 3' processing enzyme YqfG also failed to complement 16S rRNA processing in cells depleted for RNase P, we have not formally eliminated the possibility that the activity of these proteins is somehow impacted by (p)ppGpp or GTP levels. The mechanism through which tRNA depletion results in increased or decreased mRNA levels of several 30S mRNA assembly factors is currently unknown. Our preliminary data suggest that this is a mixture between transcriptional and post-transcriptional effects (data not shown) and this will be developed in detail in a later study.

The effect of RNase P and RNase Z depletion on rRNA processing is specific for the 3' end of 16S rRNA. Given the current models that all final processing steps occur post-assembly in *E. coli*, it is surprising that 5' maturation was not also affected. This may suggest some differences in the order of events between Gram-positive and negative bacteria. An earlier study showed that tRNA functional defects in *E. coli* could lead to non-specific problems with both 16S and 23S rRNA maturation, but the mechanism involved was not addressed (Slagter-Jager et al., 2007). In another study that may be related to the coupling mechanism described here, the Deutscher group showed in the 1970's that the strong growth defects of *E. coli* strains lacking nucleotidyl-transferase activity, required to repair the terminal CCA motif of tRNAs, could be suppressed by inactivation of the *relA* gene (Deutscher et al., 1977). This observation is coherent with our data that tRNA maturation defects promote the synthesis of (p)ppGpp, and potentially extends this phenomenon to Gram-negative bacteria. Coordination between tRNA processing and ribosome biogenesis has also been proposed in yeast, based on the observation that the transport factor Sxm1p ferries both the tRNA processing co-factor Lhp1p and the ribosomal proteins Rpl16p, Rpl21p and Rpll34p from the cytoplasm to the nucleoplasm (Rosenblum et al., 1997). The link between tRNA maturation and ribosome biogenesis may therefore be universally conserved, but with distinct mechanisms from one group of organisms to the next.

Acknowledgments

We thank J.D. Wang for strains lacking *ywaC, yjbM* and *relA* and advice on how to build a (p)ppGpp overproducing strain. We thank both JDW and R. Gourse for advice on how to measure (p)ppGpp levels by TLC. We thank lab members, M. Springer, C. Tisné, M. Catala, R. Britton, E. Maisonneuve and M. Cashel for helpful comments. This work was supported by funds from the CNRS (UPR 9073), Université Paris VII-Denis Diderot, the Agence Nationale de la Recherche (ARNr-QC) and the Labex (Dynamo) program. The mass spectrometry instrumentation was funded by the University of Strasbourg, IdEx "Equipement mi-lourd" 2015.

Author Contributions:

AT, JU, LG and SF performed the experiments; PH and LK performed mass spectrometry analysis. All authors participated in analysing data. CC, FB and AT wrote the paper. FB and CC are co-supervisors of PhD student AT.

Declaration of interests:

The authors declare no competing interests.

References

Amato, S.M., Orman, M.A., and Brynildsen, M.P. (2013). Metabolic control of persister formation in *Escherichia coli*. Mol Cell *50*, 475-487.

Arenz, S., Abdelshahid, M., Sohmen, D., Payoe, R., Starosta, A.L., Berninghausen, O., Hauryliuk, V., Beckmann, R., and Wilson, D.N. (2016). The stringent factor RelA adopts an open conformation on the ribosome to stimulate ppGpp synthesis. Nucleic Acids Res *44*, 6471-6481.

Baumgardt, K., Gilet, L., Figaro, S., and Condon, C. (2018). The essential nature of YqfG, a YbeY homologue required for 3' maturation of *Bacillus subtilis* 16S ribosomal RNA is suppressed by deletion of RNase R. Nucleic Acids Res *46*, 8605-8615.

Ben-Yehuda, S., Rudner, D.Z., and Losick, R. (2003). RacA, a bacterial protein that anchors chromosomes to the cell poles. Science *299*, 532-536.

Bremer, H., and Dennis, P.P. (1996). Modulation of chemical composition and other parameters of the cell by growth rate. In *Escherichia coli* and *Salmonella*: cellular and molecular biology, F.C. Neidhardt, R. Curtiss, J.L. Ingraham, E.C. Lin, K.B. Low, B. Magasanik, W.S. Reznikoff, M. Riley, M. Schaechter, and H.E. Umbarger, eds. (Washington, D.C.: American Society for Microbiology), pp. 1553-1569.

Britton, R.A., Wen, T., Schaefer, L., Pellegrini, O., Uicker, W.C., Mathy, N., Tobin, C., Daou, R., Szyk, J., and Condon, C. (2007). Maturation of the 5' end of *Bacillus subtilis* 16S rRNA by the essential ribonuclease YkqC/RNase J1. Mol Microbiol *63*, 127-138.

Brown, A., Fernandez, I.S., Gordiyenko, Y., and Ramakrishnan, V. (2016). Ribosome-dependent activation of stringent control. Nature *534*, 277-280.

Bunner, A.E., Nord, S., Wikstrom, P.M., and Williamson, J.R. (2010). The effect of ribosome assembly cofactors on *in vitro* 30S subunit reconstitution. J Mol Biol *398*, 1-7.

Bylund, G.O., Wipemo, L.C., Lundberg, L.A., and Wikstrom, P.M. (1998). RimM and RbfA are essential for efficient processing of 16S rRNA in *Escherichia coli*. J Bacteriol *180*, 73-82.

Cashel, M., and Rudd, K.E. (1987). The stringent response. In *Escherichia coli* and *Salmonella* typhimurium: Cellular and Molecular Biology, F.C. Neidhardt, ed. (Washington, D.C.: American Society for Microbiology), pp. 1410-1438.

Charollais, J., Pflieger, D., Vinh, J., Dreyfus, M., and Iost, I. (2003). The DEAD-box RNA helicase SrmB is involved in the assembly of 50S ribosomal subunits in *Escherichia coli*. Mol Microbiol *48*, 1253-1265.

Chen, S.S., and Williamson, J.R. (2013). Characterization of the ribosome biogenesis landscape in *E. coli* using quantitative mass spectrometry. J Mol Biol *425*, 767-779.

Chowdhury, N., Kwan, B.W., and Wood, T.K. (2016). Persistence increases in the absence of the alarmone guanosine tetraphosphate by reducing cell growth. Scientific reports *6*, 20519.

Condon, C. (2014). RNA Processing. In Reference Module in Biomedical Sciences (Elsevier).

Corrigan, R.M., Bellows, L.E., Wood, A., and Grundling, A. (2016). ppGpp negatively impacts ribosome assembly affecting growth and antimicrobial tolerance in Gram-positive bacteria. Proc Natl Acad Sci U S A *113*, E1710-1719.

Crary, S.M., Niranjanakumari, S., and Fierke, C.A. (1998). The protein component of *Bacillus subtilis* ribonuclease P increases catalytic efficiency by enhancing interactions with the 5' leader sequence of pre-tRNAAsp. Biochemistry *37*, 9409-9416.

Deutscher, M.P., Setlow, P., and Foulds, J. (1977). *relA* overcomes the slow growth of *cca* mutants. J Mol Biol *117*, 1095-1100.

DiChiara, J.M., Liu, B., Figaro, S., Condon, C., and Bechhofer, D.H. (2016). Mapping of internal monophosphate 5' ends of *Bacillus subtilis* messenger RNAs and ribosomal RNAs in wild-type and ribonuclease-mutant strains. Nucleic Acids Res *44*, 3373-3389.

Dunn, J.J., and Studier, F.W. (1973). T7 early RNAs and *E. coli* ribosomal RNAs are cut from large precursor RNAs *in vivo* by ribonuclease III. Proc. Natl. Acad. Sci. USA *70*, 3296-3300.

Durand, S., Gilet, L., and Condon, C. (2012). The essential function of *B. subtilis* RNase III is to silence foreign toxin genes. PLoS genetics *8*, e1003181.

Feng, B., Mandava, C.S., Guo, Q., Wang, J., Cao, W., Li, N., Zhang, Y., Zhang, Y., Wang, Z., Wu, J., *et al.* (2014). Structural and functional insights into the mode of action of a universally conserved Obg GTPase. PLoS biology *12*, e1001866.

Figaro, S., Durand, S., Gilet, L., Cayet, N., Sachse, M., and Condon, C. (2013). *Bacillus subtilis* mutants with knockouts of the genes encoding ribonucleases RNase Y and RNase J1 are viable, with major defects in cell morphology, sporulation, and competence. J Bacteriol *195*, 2340-2348.

Franco, I.S., Mota, L.J., Soares, C.M., and de Sa-Nogueira, I. (2007). Probing key DNA contacts in AraR-mediated transcriptional repression of the *Bacillus subtilis* arabinose regulon. Nucleic Acids Res *35*, 4755-4766.

Gaal, T., Bartlett, M.S., Ross, W., Turnbough, C.L., Jr., and Gourse, R.L. (1997). Transcription regulation by initiating NTP concentration: rRNA synthesis in bacteria. Science *278*, 2092-2097.

Gossringer, M., Kretschmer-Kazemi Far, R., and Hartmann, R.K. (2006). Analysis of RNase P protein (rnpA) expression in *Bacillus subtilis* utilizing strains with suppressible rnpA expression. J Bacteriol *188*, 6816-6823.

Guerout-Fleury, A.M., Frandsen, N., and Stragier, P. (1996). Plasmids for ectopic integration in *Bacillus subtilis.* Gene *180*, 57-61.

Guerout-Fleury, A.M., Shazand, K., Frandsen, N., and Stragier, P. (1995). Antibiotic-resistance cassettes for *Bacillus subtilis*. Gene *167*, 335-336.

Guerrier-Takada, C., Gardiner, K., Marsh, T., Pace, N., and Altman, S. (1983). The RNA moiety of ribonuclease P is the catalytic subunit of the enzyme. Cell *35*, 849-857.

Guo, Q., Goto, S., Chen, Y., Feng, B., Xu, Y., Muto, A., Himeno, H., Deng, H., Lei, J., and Gao, N. (2013). Dissecting the in vivo assembly of the 30S ribosomal subunit reveals the role of RimM and general features of the assembly process. Nucleic Acids Res *41*, 2609-2620.

Hase, Y., Yokoyama, S., Muto, A., and Himeno, H. (2009). Removal of a ribosome small subunit-dependent GTPase confers salt resistance on *Escherichia coli* cells. RNA *15*, 1766-1774.

Herskovitz, M.A., and Bechhofer, D.H. (2000). Endoribonuclease RNase III is essential in *Bacillus subtilis*. Mol Microbiol *38*, 1027-1033.

Hwang, J., and Inouye, M. (2006). The tandem GTPase, Der, is essential for the biogenesis of 50S ribosomal subunits in *Escherichia coli*. Mol Microbiol *61*, 1660-1672.

Jacob, A.I., Kohrer, C., Davies, B.W., RajBhandary, U.L., and Walker, G.C. (2013). Conserved bacterial RNase YbeY plays key roles in 70S ribosome quality control and 16S rRNA maturation. Mol Cell *49*, 427-438.

Kim, L., Mogk, A., and Schumann, W. (1996). A xylose-inducible *Bacillus subtilis* integration vector and its application. Gene *181*, 71-76.

Koo, B.M., Kritikos, G., Farelli, J.D., Todor, H., Tong, K., Kimsey, H., Wapinski, I., Galardini, M., Cabal, A., Peters, J.M., *et al.* (2017). Construction and Analysis of Two Genome-Scale Deletion Libraries for *Bacillus subtilis*. Cell systems *4*, 291-305 e297.

Krasny, L., and Gourse, R.L. (2004). An alternative strategy for bacterial ribosome synthesis: *Bacillus subtilis* rRNA transcription regulation. EMBO J *23*, 4473-4483.

Kriel, A., Bittner, A.N., Kim, S.H., Liu, K., Tehranchi, A.K., Zou, W.Y., Rendon, S., Chen, R., Tu, B.P., and Wang, J.D. (2012). Direct regulation of GTP homeostasis by (p)ppGpp: a critical component of viability and stress resistance. Mol Cell *48*, 231-241.

Leong, V., Kent, M., Jomaa, A., and Ortega, J. (2013). *Escherichia coli rimM* and *yjeQ* null strains accumulate immature 30S subunits of similar structure and protein complement. RNA *19*, 789-802.

Li, Z., Pandit, S., and Deutscher, M.P. (1998). Polyadenylation of stable RNA precursors *in vivo*. Proc Natl Acad Sci U S A *95*, 12158-12162.

Liu, K., Myers, A.R., Pisithkul, T., Claas, K.R., Satyshur, K.A., Amador-Noguez, D., Keck, J.L., and Wang, J.D. (2015). Molecular mechanism and evolution of guanylate kinase regulation by (p)ppGpp. Mol Cell *57*, 735-749.

Loh, P.C., Morimoto, T., Matsuo, Y., Oshima, T., and Ogasawara, N. (2007). The GTP-binding protein YqeH participates in biogenesis of the 30S ribosome subunit in *Bacillus subtilis*. Genes Genet Syst *82*, 281-289.

Loveland, A.B., Bah, E., Madireddy, R., Zhang, Y., Brilot, A.F., Grigorieff, N., and Korostelev, A.A. (2016). Ribosome*RelA structures reveal the mechanism of stringent response activation. eLife *5*.

Mathy, N., Benard, L., Pellegrini, O., Daou, R., Wen, T., and Condon, C. (2007). 5'-to-3' exoribonuclease activity in bacteria: role of RNase J1 in rRNA maturation and 5' stability of mRNA. Cell *129*, 681-692.

Miller, D.L., Cashel, M., and Weissbach, H. (1973). The interaction of guanosine 5'-diphosphate, 2' (3')-diphosphate with the bacterial elongation factor Tu. Arch Biochem Biophys *154*, 675-682.

Milon, P., Tischenko, E., Tomsic, J., Caserta, E., Folkers, G., La Teana, A., Rodnina, M.V., Pon, C.L., Boelens, R., and Gualerzi, C.O. (2006). The nucleotide-binding site of bacterial translation initiation factor 2 (IF2) as a metabolic sensor. Proc Natl Acad Sci U S A *103*, 13962-13967.

Mitkevich, V.A., Ermakov, A., Kulikova, A.A., Tankov, S., Shyp, V., Soosaar, A., Tenson, T., Makarov, A.A., Ehrenberg, M., and Hauryliuk, V. (2010). Thermodynamic characterization of ppGpp binding to EF-G or IF2 and of initiator tRNA binding to free IF2 in the presence of GDP, GTP, or ppGpp. J Mol Biol *402*, 838-846.

My, L., Ghandour Achkar, N., Viala, J.P., and Bouveret, E. (2015). Reassessment of the Genetic Regulation of Fatty Acid Synthesis in *Escherichia coli*: Global Positive Control by the Dual Functional Regulator FadR. J Bacteriol *197*, 1862-1872.

Natori, Y., Tagami, K., Murakami, K., Yoshida, S., Tanigawa, O., Moh, Y., Masuda, K., Wada, T., Suzuki, S., Nanamiya, H., *et al.* (2009). Transcription activity of individual *rrn* operons in

Bacillus subtilis mutants deficient in (p)ppGpp synthetase genes, *relA*, *yjbM*, and *ywaC*. J Bacteriol *191*, 4555-4561.

Nicolas, P., Mader, U., Dervyn, E., Rochat, T., Leduc, A., Pigeonneau, N., Bidnenko, E., Marchadier, E., Hoebeke, M., Aymerich, S., *et al.* (2012). Condition-dependent transcriptome reveals high-level regulatory architecture in *Bacillus subtilis*. Science *335*, 1103-1106.

Noller, H.F., and Nomura, M. (1987). Ribosomes. In Escherichia coli and Salmonella typhimurium: Cellular and Molecular Biology, F.C. Neidhardt, J.L. Ingraham, K.B. Low, B. Magasanik, M. Schaechter, and H.E. Umbarger, eds. (Washington, D.C.: ASM Press), pp. 104-126.

Nord, S., Bylund, G.O., Lovgren, J.M., and Wikstrom, P.M. (2009). The RimP protein is important for maturation of the 30S ribosomal subunit. J Mol Biol *386*, 742-753.

Pao, C.C., and Gallant, J. (1978). A gene involved in the metabolic control of ppGpp synthesis. Mol Gen Genet *158*, 271-277.

Pellegrini, O., Li de la Sierra-Gallay, I., Piton, J., Gilet, L., and Condon, C. (2012). Activation of tRNA maturation by downstream uracil residues in *B. subtilis*. Structure *20*, 1769-1777.

Pellegrini, O., Nezzar, J., Marchfelder, A., Putzer, H., and Condon, C. (2003). Endonucleolytic processing of CCA-less tRNA precursors by RNase Z in *Bacillus subtilis*. EMBO J. *22*, 4534-4543.

Peters, J.M., Colavin, A., Shi, H., Czarny, T.L., Larson, M.H., Wong, S., Hawkins, J.S., Lu, C.H.S., Koo, B.M., Marta, E., *et al.* (2016). A comprehensive, CRISPR-based functional analysis of essential genes in bacteria. Cell *165*, 1493-1506.

Polakis, S.E., Guchhait, R.B., and Lane, M.D. (1973). Stringent control of fatty acid synthesis in *Escherichia coli*. Possible regulation of acetyl coenzyme A carboxylase by ppGpp. J Biol Chem *248*, 7957-7966.

Redko, Y., Bechhofer, D.H., and Condon, C. (2008). Mini-III, an unusual member of the RNase III family of enzymes, catalyses 23S ribosomal RNA maturation in *B. subtilis*. Mol Microbiol *68*, 1096-1106.

Reich, C., Olsen, G.J., Pace, B., and Pace, N.R. (1988). Role of the protein moiety of ribonuclease P, a ribonucleoprotein enzyme. Science *239*, 178-181.

Rosenblum, J.S., Pemberton, L.F., and Blobel, G. (1997). A nuclear import pathway for a protein involved in tRNA maturation. J Cell Biol *139*, 1655-1661.

Ross, W., Sanchez-Vazquez, P., Chen, A.Y., Lee, J.H., Burgos, H.L., and Gourse, R.L. (2016). ppGpp binding to a site at the RNAP-DksA interface accounts for its dramatic effects on transcription initiation during the stringent response. Mol Cell *62*, 811-823.

Sayed, A., Matsuyama, S., and Inouye, M. (1999). Era, an essential *Escherichia coli* small G-protein, binds to the 30S ribosomal subunit. Biochem Biophys Res Commun *264*, 51-54.

Shajani, Z., Sykes, M.T., and Williamson, J.R. (2011). Assembly of bacterial ribosomes. Annu Rev Biochem *80*, 501-526.

Shetty, S., and Varshney, U. (2016). An evolutionarily conserved element in initiator tRNAs prompts ultimate steps in ribosome maturation. Proc Natl Acad Sci U S A *113*, E6126-E6134.

Slagter-Jager, J.G., Puzis, L., Gutgsell, N.S., Belfort, M., and Jain, C. (2007). Functional defects in transfer RNAs lead to the accumulation of ribosomal RNA precursors. RNA *13*, 597-605.

Sprinzl, M., and Richter, D. (1976). Free 3'-OH group of the terminal adenosine of the tRNA molecule is essential for the synthesis in vitro of guanosine tetraphosphate and pentaphosphate in a ribosomal system from *Escherichia coli*. Eur J Biochem *71*, 171-176.

Steinmetz, M., and Richter, R. (1994). Plasmids designed to alter the antibiotic resistance expressed by insertion mutations in *Bacillus subtilis*, through in vivo recombination. Gene *142*, 79-83.

Stent, G.S., and Brenner, S. (1961). A genetic locus for the regulation of ribonucleic acid synthesis. Proc Natl Acad Sci U S A *47*, 2005-2014.

Toymentseva, A.A., Schrecke, K., Sharipova, M.R., and Mascher, T. (2012). The LIKE system, a novel protein expression toolbox for *Bacillus subtilis* based on the liaI promoter. Microb Cell Fact *11*, 143.

Traxler, M.F., Summers, S.M., Nguyen, H.T., Zacharia, V.M., Hightower, G.A., Smith, J.T., and Conway, T. (2008). The global, ppGpp-mediated stringent response to amino acid starvation in *Escherichia coli*. Mol Microbiol *68*, 1128-1148.

Uicker, W.C., Schaefer, L., Koenigsknecht, M., and Britton, R.A. (2007). The essential GTPase YqeH is required for proper ribosome assembly in *Bacillus subtilis*. J Bacteriol *189*, 2926-2929.

Wang, J.D., Sanders, G.M., and Grossman, A.D. (2007). Nutritional control of elongation of DNA replication by (p)ppGpp. Cell *128*, 865-875.

Waugh, D.S., and Pace, N.R. (1990). Complementation of an RNase P RNA (*rnpB*) gene deletion in *Escherichia coli* by homologous genes from distantly related eubacteria. J Bacteriol *172*, 6316-6322.

Wegscheid, B., Condon, C., and Hartmann, R.K. (2006). Type A and B RNase P RNAs are interchangeable in vivo despite substantial biophysical differences. EMBO Rep *7*, 411-417.

Wen, T., Oussenko, I.A., Pellegrini, O., Bechhofer, D.H., and Condon, C. (2005). Ribonuclease PH plays a major role in the exonucleolytic maturation of CCA-containing tRNA precursors in *Bacillus subtilis*. Nucleic Acids Res *33*, 3636-3643.

Wendrich, T.M., and Marahiel, M.A. (1997). Cloning and characterization of a *relA/spoT* homologue from *Bacillus subtilis*. Mol Microbiol *26*, 65-79.

Figure Legends

Figure 1. Depletion of tRNA processing enzymes results in a defect in 3' processing of 16S rRNA. (A) Schematic of 16S rRNA (*rrnW*) precursor showing mature sequence in green, precursor sequences in black and key processing reactions in red. (B) and (C) Northern blots showing the effect of depleting RNase P (*rnpB* or *rnpA*) and RNase Z (*rnz*), respectively, on accumulation of the 65 nt 3' processing product. 5 μg of total RNA was probed with oligo CC172 (Table S1), specific for the 16S rRNA 3' precursor, on agarose gels (upper panel) and polyacrylamide gels (lower panel) for optimal transfer of the ~1620 nt and 65 nt species, respectively. The histograms show the calculation of processing efficiency (65-nt/pre-16S) for each strain, normalized to wt (n=4 *rnpB* and *rnpA*; n=3 *rnz*; n=7 wt). The fold differences in processing efficiencies between depleted and non-depleted strains are indicated on each histogram.

Figure 2. Depletion of tRNA processing enzymes results in perturbed expression of genes involved in 30S ribosome biogenesis. (A) Northern blots showing the effects of Δ*ksgA,* Δ*ylxS (rimP),* Δ*rbfA,* Δ*ydaF (rimJ1),* Δ*yjcK (rimJ2)* deletions and Era depletion (in 168 *trpC2* background) on 16S rRNA 3' processing efficiency. (B) Northern blot showing the effects of YqfG depletion and Δ*rpsU* (S21) Δ*rimM,* Δ*cpgA,* Δ*yqeH* deletions (in W168 background) on 16S rRNA 3' processing efficiency. The histograms show the calculation of processing efficiency (65-nt/pre-16S) for each strain, normalized to wt (n=2). (C) Northern blots showing up-regulation of *era* (probe CC1846) and *yqeH* (probe CC1847) expression in strains depleted for RNase P (*Pxyl-rnpA* and *Pspac-rnpB*) and RNase Z (*Pspac-rnz*). (D) Northern blots showing down-regulation of *rimM* (probe CC1845) and *cpgA* (riboprobe) expression in the same depletion strains.

Figure 3. Effect of RNase P and Z depletions on ribosome assembly (A) Sucrose gradients in 3 mM Mg of wt, *Pxyl-rnpA* and *Pspac-rnz* depletion strains grown in the absence of inducer. (B) 16S rRNA profile in sucrose gradients from panel (A). (C) LC-MS/MS analysis (n=3) of pre-30S fractions in wt vs *Pxyl-rnpA* and *Pspac-rnz* depletion strains grown in the absence of inducer. The number of spectra for each protein were first normalized to the total spectra observed in each

fraction and then normalized to the equivalent number in wt. The percent fill of each box represents the amount of each ribosomal protein compared to wt. Proteins shown in red are represented at ≤ 10%; orange >10% but ≤ 50% of wt; green > 50% of wt. Assembly map is from (Chen and Williamson, 2013).

Figure 4. Depletion of tRNA processing enzymes leads to induction of the stringent response. (A) Depletion of tRNA processing enzymes leads to the production of (p)ppGpp. Thin layer chromatography (TLC) analysis of ^{32}P-labelled nucleotides extracted from *Pspac-rnpB, Pxyl-rnpA* and *Pspac-rnz* depletion strains grown in the absence of inducer. Arginine hydroxamate (RHX, 250 µg/mL) was added to wt cultures and strains unable to make (p)ppGpp (ppGpp^0) as positive and negative controls. Note that the top and bottom halves of the chromatogram are exposed for different times. (B) Defects in tRNA processing cause derepression of the CodY regulon. Northern blot showing derepression of *ilvA* and *ywaA* gene expression in *Pspac-rnpB, Pxyl-rnpA* and *Pspac-rnz* depletion strains growing in the presence and absence of inducer. (C) Derepression of the CodY-regulated *ywaA* mRNA in *rnpA*-depleted strains is RelA-dependent. Northern blot showing *ywaA* gene expression in the *Pxyl-rnpA* depletion strains growing in the presence and absence of xylose in wt, *yjbM ywaC* double mutant and *yjbM ywaC relA* triple mutant (ppGpp^0) genetic backgrounds.

Figure 5. 16S rRNA 3' processing is partially restored in RNase P-depleted cells in a ppGpp^0 background. Northern blot comparing the effect of depleting RNase P (*rnpA* or *rnpB*) in a ppGpp+ and ppGpp^0 background on the accumulation of the 65 nt 3' processing product. The fold differences in processing efficiencies, normalized to wt, between depleted and non-depleted strains are indicated underneath the Northern blots (n=4 *rnpB* and *rnpA*; n=3 *rnz*; n=2 *rnpB* ppGpp^0 and *rnpA* ppGpp^0, n=7 wt).

Figure 6. Increased (p)ppGpp synthesis and decreased GTP levels inhibit 16S rRNA 3' processing in the absence of tRNA processing defects. (A) Induction of the stringent response by amino acid starvation results in defects in 16S rRNA 3' processing. Northern blots performed on total RNA after addition of arginine hydroxamate (RHX; 250 µg/mL) to wt cultures at times indicated. Quantification of processing efficiency (65-nt/full-length) is calculated underneath the

Northern blots, normalized to the untreated sample (n=2). The blot in the top panel was reprobed with oligo CC2213 specific for the CodY-regulated *ywaA* gene. (B)+(C) Induction of (p)ppGpp synthesis is sufficient to cause defects in 16S rRNA 3' processing. (B) TLC showing production of (p)ppGpp in *ywaC yjbM relA* strains expressing *ywaC* under control of the xylose promoter in the *amyE* locus 30 mins after addition of RHX (250 µg/mL) to cell cultures. (C) Northern blot performed on total RNA after addition of xylose (2%) to *ywaC yjbM relA* strains expressing *ywaC* under control of the xylose promoter at times indicated (n=2). (D) Inhibition of GTP synthesis results in defects in 16S rRNA 3' processing. Northern blot performed on total RNA after addition of decoyinine (dec; 500 µg/mL) to wt cultures at times indicated (n=2).

Figure 7. Model for coupling of tRNA and 16S rRNA 3' processing. Precursor tRNAs (green) and RelA occupy the A-site of the ribosome and provoke synthesis of (p)ppGpp. Upward pointing green arrows show increased synthesis or activity, downward pointing red arrows show decreases. Increased (p)ppGpp levels inhibit the synthesis of GTP by binding to Gmk and HprT (Kriel et al., 2012), leading to derepression of the CodY regulon, and potentially inhibit the GTPase activity of Era and CpgA (Corrigan et al., 2016). The decreased GTP pools may also affect the GTPase activity of Era, CpgA and YqeH, resulting in late 30S assembly defects, represented by the absence of ribosomal proteins S2, S3, S5, S14, S19 and S21. The assembly defect in turn leads to a defect in 16S rRNA 3' processing. It is also possible that perturbation of expression of 30S assembly factors contributes to the assembly defect upon accumulation of tRNA precursors.

STAR METHODS

CONTACT FOR REAGENT AND RESOURCE SHARING

Further information and requests for resources and reagents should be directed to and will be fulfilled by the Lead Contact Ciarán Condon (condon@ibpc.fr).

EXPERIMENTAL MODEL AND SUBJECT DETAILS

B. subtilis strain W168 and *B. subtilis 168 trpC*. All mutant strains used were derived from these two parental strains, by transformation with PCR products, plasmids or chromosomal DNA from both previously published strains or new constructs. A list of all strains used is provided in Table S1. Details of new strains and plasmid constructs are provided in Tables S2 and S4, respectively.

METHOD DETAILS

Bacterial cultures

All cultures were grown in 2xYT medium. Overnight cultures were grown in the presence of appropriate antibiotics. Experimental cultures did not contain antibiotics, except when necessary for maintaining plasmids. For depletion studies, overnight cultures grown in the presence of inducer (1 mM IPTG or 2% xylose) were washed three times in an equal volume of pre-warmed medium and inoculated into fresh medium with or without inducer at OD_{600} = 0.05 (*rnpA* and *rnz*) or 0.2 (*rnpB*), the empirically determined optimal depletion conditions for the respective strains. For the depletion of RnpA, cells were inoculated into fresh medium containing glucose (2%) to tighten repression of the *Pxyl* promoter. Cultures were followed until they reached a plateau, typically around OD_{600}=0.6 for *rnpA* and *rnz*, and 0.3 for *rnpB*, and harvested for RNA preparation.

For amino acid starvation, arginine hydroxamate (RHX) was added at 250 μg/mL at $0D_{600}$ = 0.3. For inhibition of GTP synthesis, decoyinine was dissolved at 1 mg/mL in 2xYT pre-warmed to 37°C and an equal volume added to 1 mL cultures at OD_{600} = 0.6 (final concentration 500 μg/mL). For the CRISPRi strain targeting *era* expression, cells were grown overnight in 2xYT and diluted in the presence or absence of 1% xylose. Cells were grown to OD_{600} = 0.5 before harvesting.

RNA isolation and Northern blots

RNA was typically isolated from 1 mL mid-log phase *B. subtilis* cells growing in 2xYT medium by the glass beads/phenol, a modification of the method described in (Bechhofer et al., 2008). For strains that plateau at very low OD_{600}, e.g. the *rnpB* depletion strain, greater volumes of cell culture (up to 8 mL) were harvested. Frozen cell pellets were resuspended in 200 µL ice-cold TE-Buffer (10 mM Tris, pH 7.5, 1 mM EDTA) and transferred to a tube containing 25 µL chloroform, 6.25 µL 20% SDS and 100 µL glass beads for lysis by three 1 min vortexing steps at max speed on a Disruptor Genie (Scientific Industries) separated with 1 min intervals on ice. After centrifugation, the supernatant was transferred to 200 µL water-saturated phenol on ice and vortexed again (with the same vortexing protocol as above) before being centrifuged for 10 min at 16,000 x g at 4°C. The supernatant was then mixed with 200 µL water-saturated phenol and 100 µL chloroform, vortexed for 1 min at full speed and centrifuged again for 10 min at 16,000 x g at 4°C. RNA was precipitated at -20°C by adding 3 volumes of 95% ethanol stored at -20°C and 0.1 volumes of 10M LiCl before being washed, dried and resuspended in 50 µL water. For Northern blots, 5 µg total RNA was run on 1% agarose or 5% acrylamide gels and transferred to hybond-N membranes (GE-Healthcare), by capillary transfer or electrotransfer, respectively. Hybridization was performed using 5′-labeled oligonucleotides using Ultra-Hyb (Life Technologies) or Roti-Hybri-Quick (Roth) hybridization buffers at 42°C for a minimum of 4 hours. Membranes were washed twice in 2×SSC 0.1% SDS (once rapidly at room temperature (RT), once for 5 min at 42°C) and then twice for 5 mins in 0.2×SSC 0.1% SDS at 42°C, as described in (Durand et al., 2012).

Primer extension

Primer extension assays were done using a modified version of the protocol described in (Britton et al., 2007) on total *B. subtilis* RNA extracted as described above, but with an additional treatment with DNase I to remove chromosomal DNA. 0.5 pmol of 5'-labeled (^{32}P) oligonucleotides was added to 5 µg of RNA in 5 µl final volume RT buffer (50 mM Tris-HCl, pH 8.3, 10 mM $MgCl_2$, 80 mM KCl) and denatured at 75°C for 4 min. The denatured mixture was frozen on dry ice for 2 mins and then transferred to ice to thaw. Oligonucleotides CC058 and CC257 were used to assay 5' processing of 16S and 23S rRNAs, respectively. A 5.2 µL mix

containing 2 mM each dNTP, 8 mM dithiothreitol (DTT), 4 units AMV reverse transcriptase (NEB) in RT buffer was then added. Reaction mixtures were incubated for 30 min at 45°C, stopped with 5 µL of 95% formamide, 20 mM EDTA, 0.05% bromophenol blue, 0.05% xylene cyanol and loaded on 5% sequencing gels.

Sucrose gradients

B. subtilis 30S and 50S ribosomal particles were separated from 50 mL of log phase *B. subtilis* cells (OD_{600} = 0.5). Cells were centrifuged and resuspended in 1 mL ice cold Buffer A (20 mM Tris-HCl pH 7.5, 200 mM NH_4Cl, 6 mM β-Mercaptoethanol) containing 3 mM $MgCl_2$ and 4 µg/mL DNase I and lysed by two passages in an ice-cold French Press (Glen Mills) at 20,000 psi. The lysate was cleared at 13,200 rpm for 30 mins at 4°C in a bench top centrifuge. A maximum of 500 µL of lysate was loaded on a 10-30% sucrose gradient in Buffer A containing 3 mM $MgCl_2$ and centrifuged at 23,000 rpm for 16h at 4°C in an SW41 rotor (Beckmann). 500 µL fractions were collected using a Piston Gradient Fractionator (Biocomp) for analysis on agarose gels or mass spectrometry. 70S ribosomes were prepared similarly but with Buffer A containing 10 mM $MgCl_2$ and centrifugation at 18,600 rpm for 16h.

Mass spectrometry analysis and data processing

Mass-spectrometry analysis was performed in triplicate. Proteins in sucrose gradient fractions were digested with sequencing-grade trypsin (Promega, Fitchburg, MA, USA). Each fraction (500 ng of digested peptides) was further analyzed by nanoLC-MS/MS on a QExactive+ mass spectrometer coupled to an EASY-nanoLC-1000 (Thermo-Fisher Scientific, USA) as described previously (Chicher et al., 2015). Data were searched against the *Bacillus subtilis* SwissProt sub-database with a decoy strategy (SwissProt release 2017_09, taxon 224308, 4294 forward protein sequences). Peptides and proteins were identified with Mascot algorithm (version 2.5, Matrix Science, London, UK) and data were further imported into Proline v1.4 software (http://proline.profiproteomics.fr/). Proteins were validated on Mascot pretty rank equal to 1, Mascot score above 25, and 1% FDR on both peptide spectrum matches (PSM score) and protein sets (Protein Set score). Proline package was further used to align proteins across all samples and to compute the Spectrum Counting values. The total number of MS/MS fragmentation spectra was used to relatively quantify each protein across all samples. The number of spectra for each

30S ribosomal protein was first normalized to the total number of spectra identified in each mutant sample and then normalized to the equivalent value obtained for the wt. Raw and processed data are given in Table S5. The % occurrence of each ribosomal protein compared to wt is reported as a % fill of the relevant box on the assembly maps shown in Figs. 3 and S3.

(p)ppGpp measurement

Synthesis of (p)ppGpp was measured with a protocol adapted from (Wang et al., 2007). $KH_2{}^{32}PO_4$ (1mCi/ml; Perkin Elmer) was added to depletion cultures growing in 2xYT a final concentration of 100 μCi/ml at OD_{600} ≈0.1 (or from the beginning in the case of *rnpB*). At OD_{600} =0.5 (or ≈0.3 for the *rnpB* depletion strain) 250 μL of culture was mixed with 55 μL 2M ice-cold formic acid and frozen on dry ice. Samples were left on ice for 20 mins and centrifuged at 4°C for 15 mins to collect the supernatant. PEI-cellulose TLC plates (J.T.Baker) were prepared by sequential immersion in distilled H_2O, air drying, immersion in methanol and a second air-drying step. Then, 20 μL of extracts were spotted progressively (2 uL at a time, dried by hairdryer on cold setting) on the plate and plates were developed in 1.5 M KH_2PO_4 (pH=3.4) as described in (Schneider et al., 2003). The region of the plate containing the unincorporated label was cut off before overnight exposure to PhosphorImager screens and scanning using a GE Typhoon scanner.

QUANTIFICATION AND STATISTICAL ANALYSIS

Northern blots were scanned using a GE Typhoon scanner. The resulting (.gel) image was quantified by drawing rectangles around individual bands using Fiji software. Processing efficiency was calculated from the ratio of the 65-nt species to the pre-16S species and normalized to the ratios calculated for the wt samples present on each gel. Experiments were performed at least in duplicate (the actual number of repetitions is given in the legend to each figure). Standard errors were calculated in Microsoft Excel.

DATA AND SOFTWARE AVAILABILITY

Raw and processed data for the mass-spectrometry experiment are given in Table S5. Raw imaging data (e.g. uncropped, unannotated agarose gels, Northern blots and thin layer chromatography autoradiograms) corresponding to individual figure panels have been deposited

in Mendeley Data (https://data.mendeley.com/datasets/d4wrkvdtjp/draft?a=ebd603ac-8c8f-4a7e-93e7-91668fe87f5c).

KEY RESOURCES TABLE

REAGENT or RESOURCE	SOURCE	IDENTIFIER
Bacterial and Virus Strains		
See Table S1 for *Bacillus subtilis* strains used in this study and Table S2 for details on new constructs.	N/A	N/A
Chemicals, Peptides, and Recombinant Proteins		
[P32] $KH_2{}^{32}PO_4$ (1mCi/ml)	Perkin-Elmer	Cat#NEX063001MC
ATP, [γ-32P]- 3000Ci/mmol 10mCi/ml EasyTide	Perkin-Elmer	Cat#BLU502A500UC
UTP, [α-32P]- 3000Ci/mmol 10mCi/ml EasyTide	Perkin-Elmer	Cat#BLU507H500UC
Decoyinine (Augustmycin A)	Abcam	Cat#ab144238
L-Arginine hydroxamate hydrochloride	Sigma-Aldrich	Cat#A7380
Bacitracin from *Bacillus licheniformis*, ≥60000 U/g (Potency)	Sigma-Aldrich	Cat#11702
Formic acid (≥97%)	MP biomedicals	Cat#0215116290
Sequencing grade modified trypsin	Promega	Cat#V5111
DNase I	Sigma-Aldrich	Cat#DN25
RNase A	Sigma-Aldrich	Cat#R6513
Set of dATP, dCTP, dGTP and dTTP	Promega	Cat#U1240
rATP, rCTP, rGTP and rUTP	Promega	Cat#E6011, E6041, E6031, E6021
Roti Hybri Quick	Roth	Cat#A981.1
Ultrahyb	Life technologies	Cat#AM8669
Aquaphenol water-saturated	MP biomedicals	Cat#AQUAPH01
AMV Reverse Transriptase	New England Biolabs	Cat#M0277
Deposited Data		
Mendeley raw imaging data (e.g. uncropped and unannotated agarose gels, Northern blots and thin layer chromatography autoradiograms).	This work	https://data.mendeley.com/datasets/d4wrkvdtjp/draft?a=ebd603ac-8c8f-4a7e-93e7-91668fe87f5c
Oligonucleotides		
See Table S3 for list of primers used in this study	N/A	N/A
Recombinant DNA		
See Table S4 for list of plasmids used in this study.	N/A	N/A
Software and Algorithms		
Pymol 2.3.0	Schrödinger	RRID: SCR_000305
Fiji	https://fiji.sc/	RRID: SCR_002285
Proline v1.4	http://proline.profiproteomics.fr/	N/A
Mascot v2.5	Matrix Science, London, UK	N/A
Other		
QExactive+ mass spectrometer	Thermo-Fisher Scientific, USA	N/A
EASY-nanoLC-1000	Thermo-Fisher Scientific, USA	N/A
French Press	Glen Mills, USA	N/A

PhosphorImager screens	GE HealthCare Life Sciences	N/A
Typhoon scanner	GE HealthCare Life Sciences	N/A
Glass beads acid-washed	Sigma-Aldrich	Cat#G1145
Piston Gradient Fractionator	Biocomp	N/A
Gradient Master	Biocomp	N/A
Membrane Amersham Hybond-N+	GE HealthCare Life Sciences	Cat#RPN203B
PEI Cellulose TLC plate, Baker-flex	J.T.Baker	Cat#2002564
Disruptor Genie Digital Cell Disruptor	Thermo-Fisher Scientific, USA	Cat#15577345

Figure 1

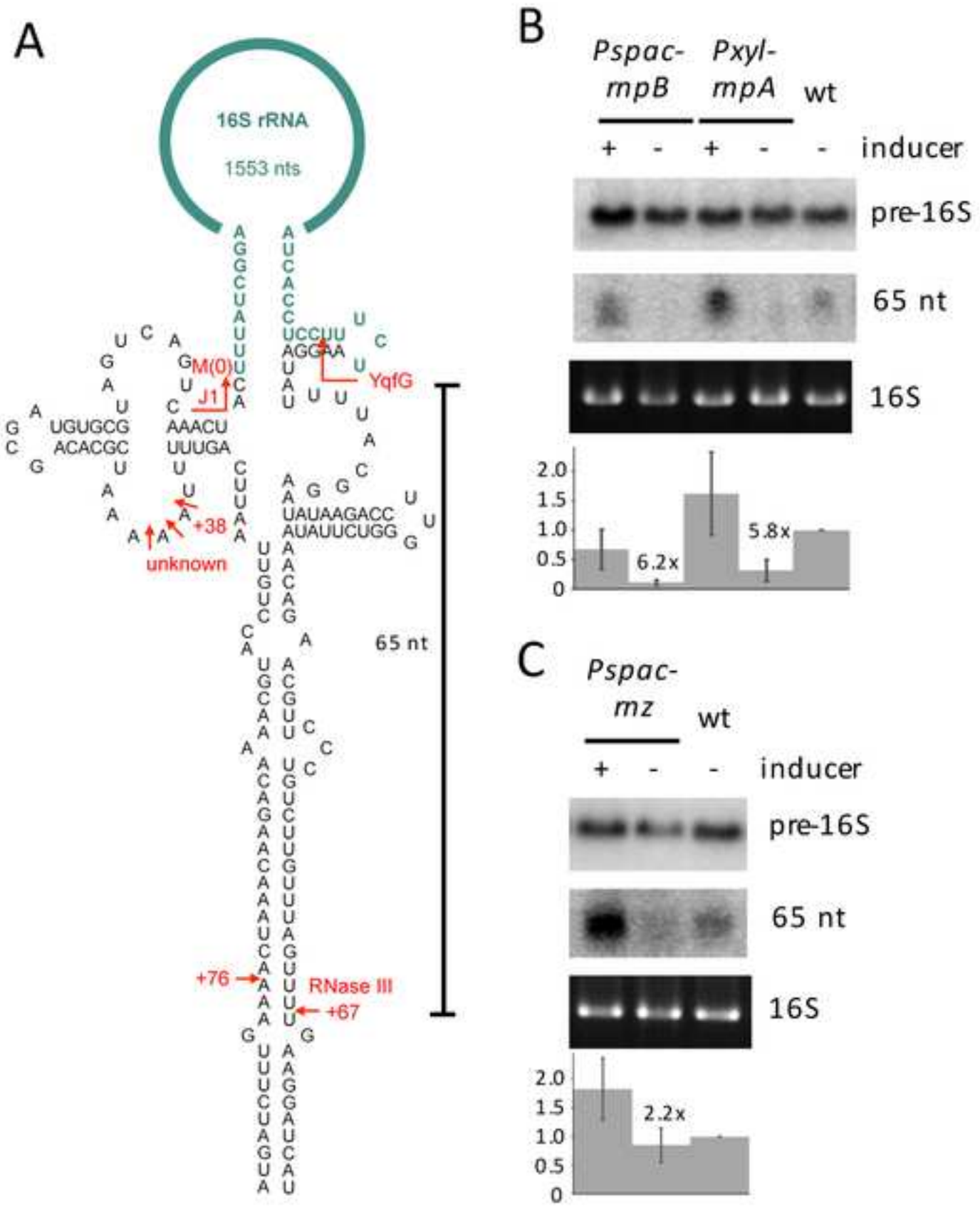

Figure 2

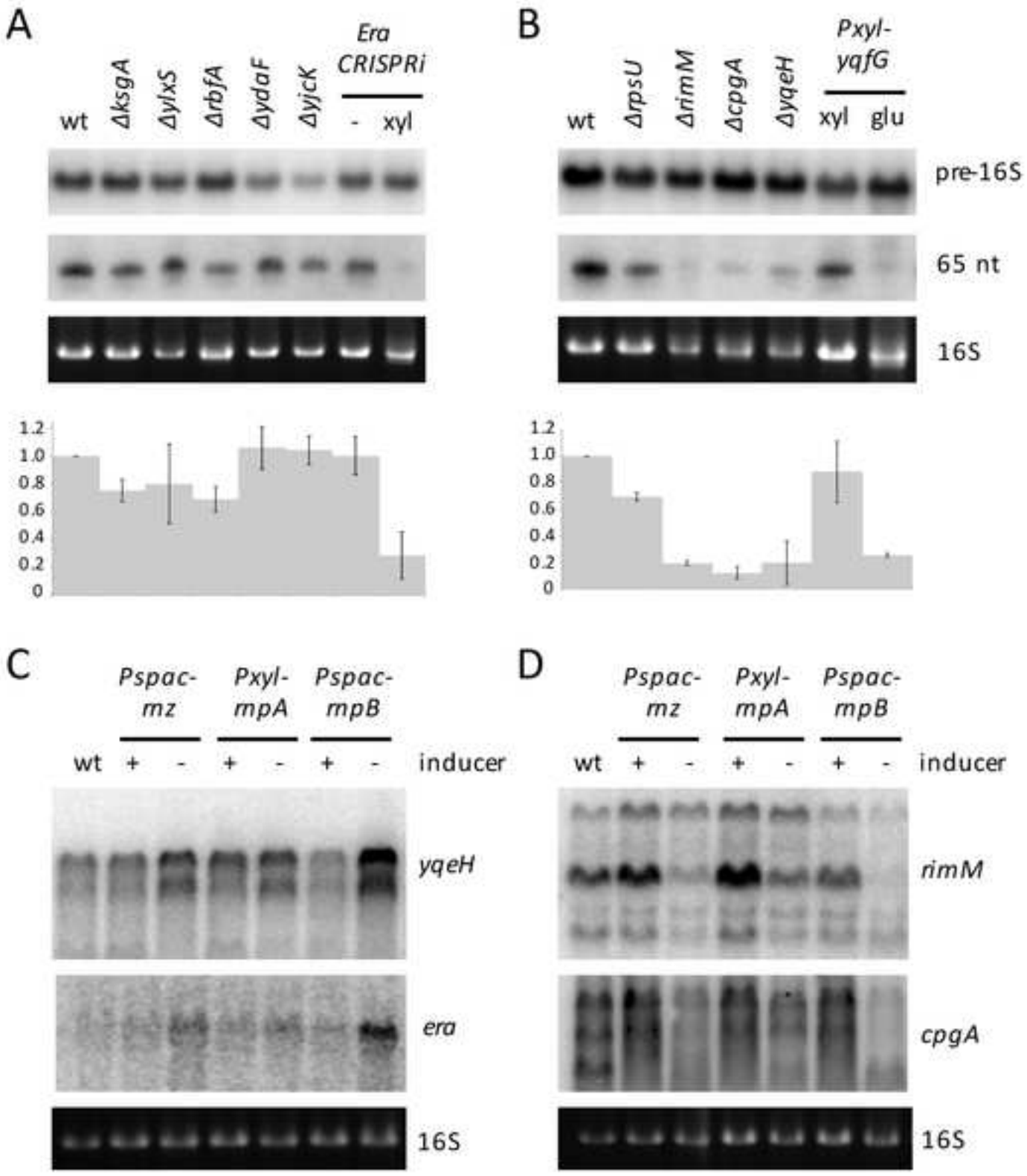

Figure 3

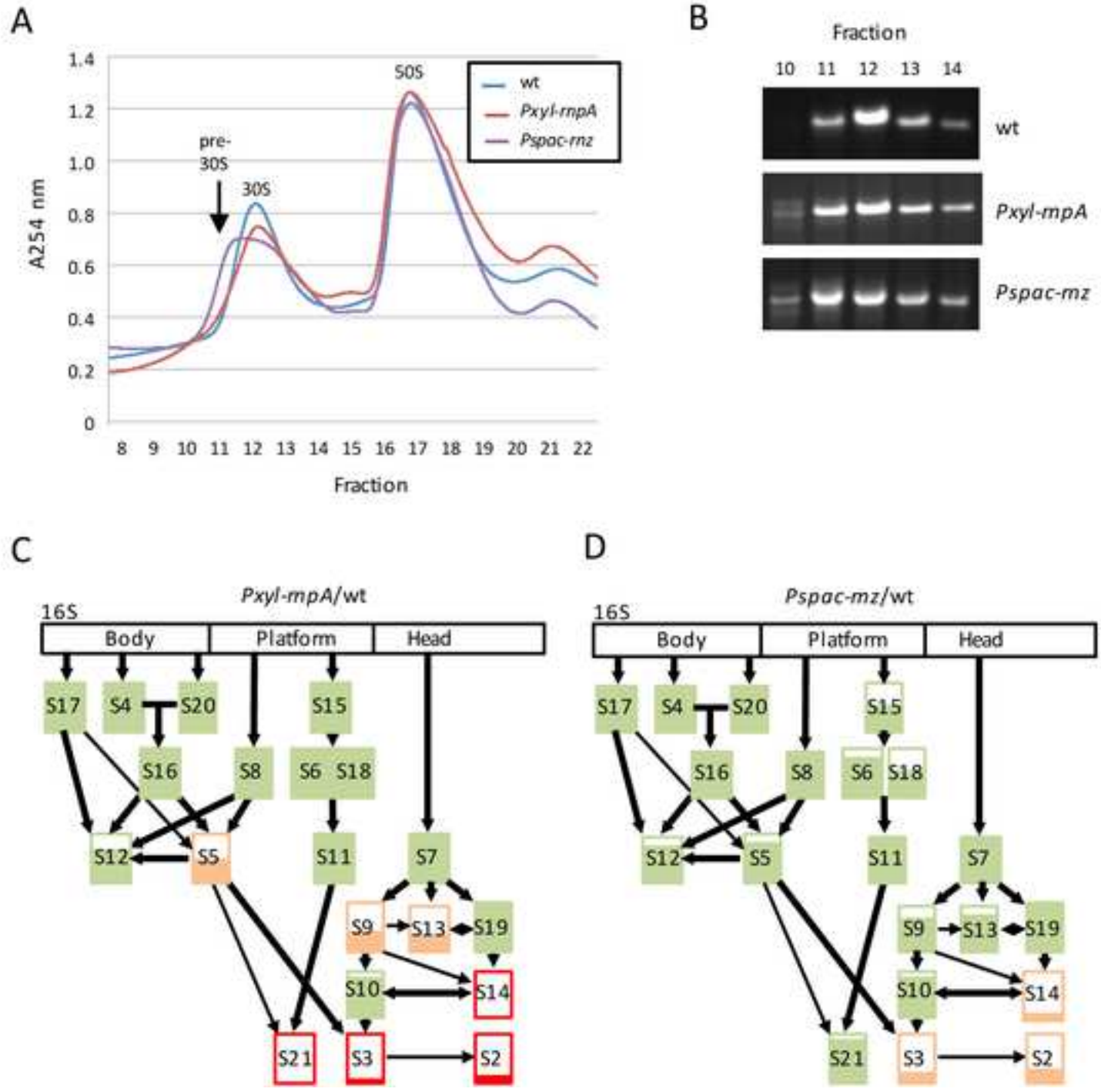

Figure 4

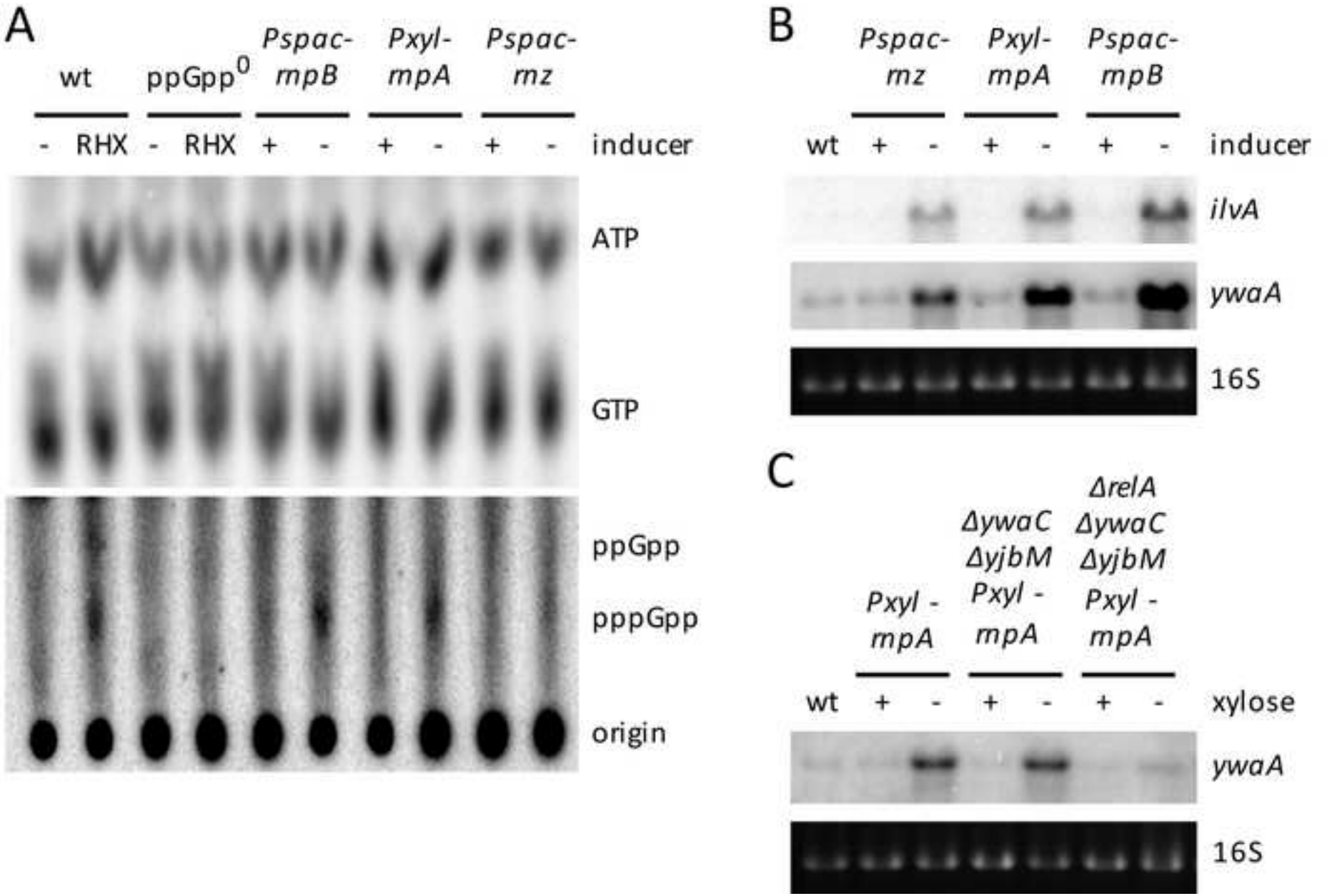

Figure 5

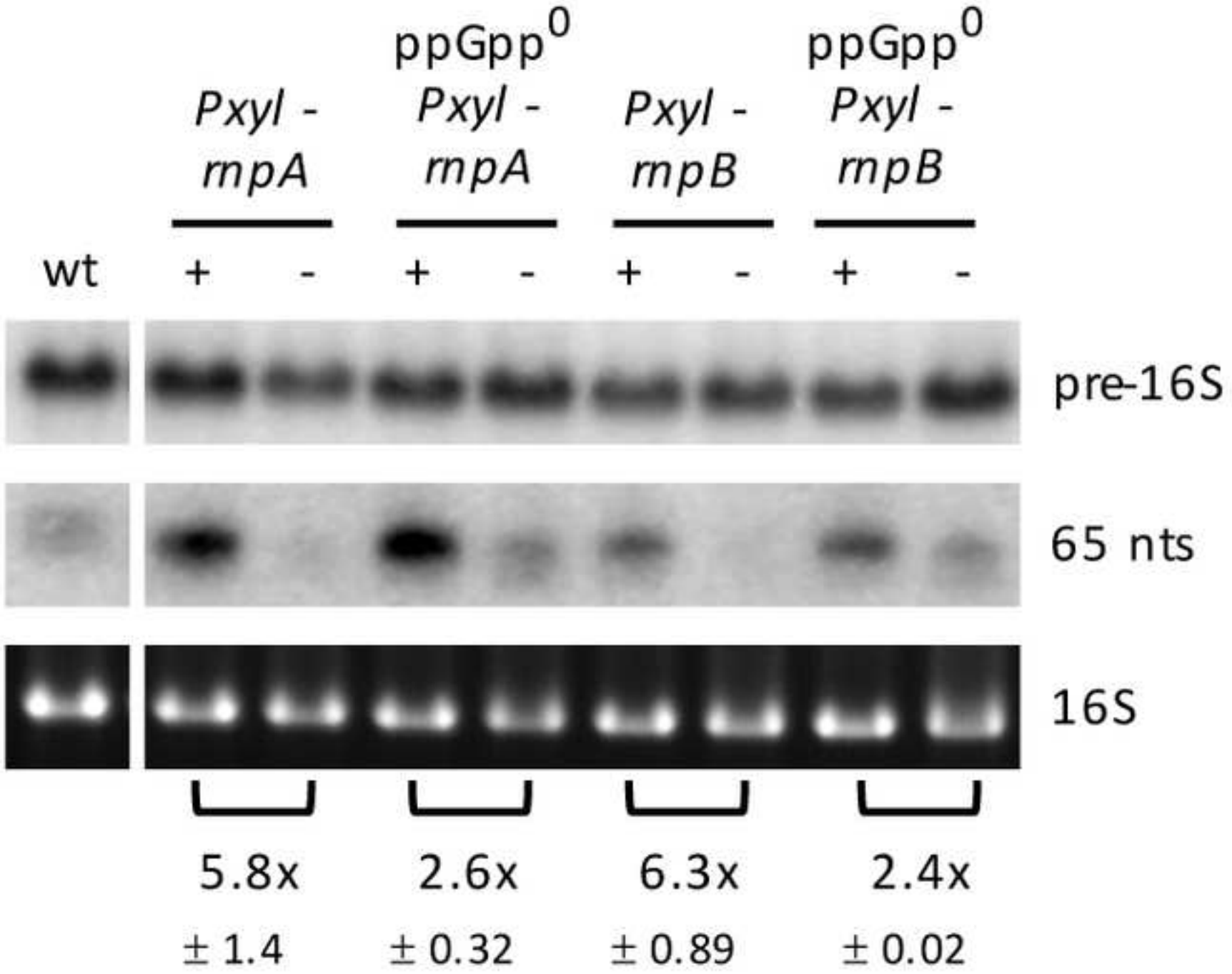

Figure 6

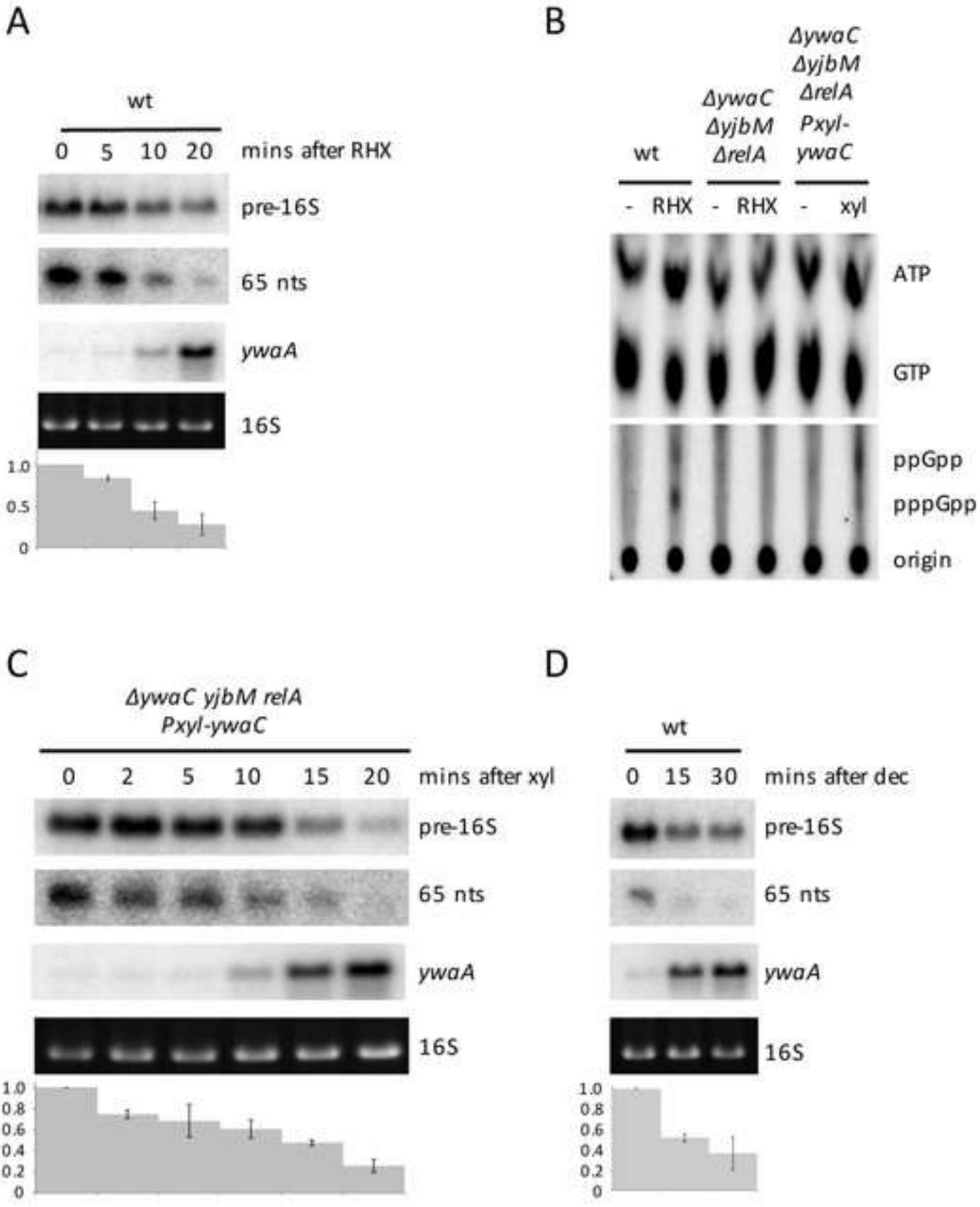

Figure 7

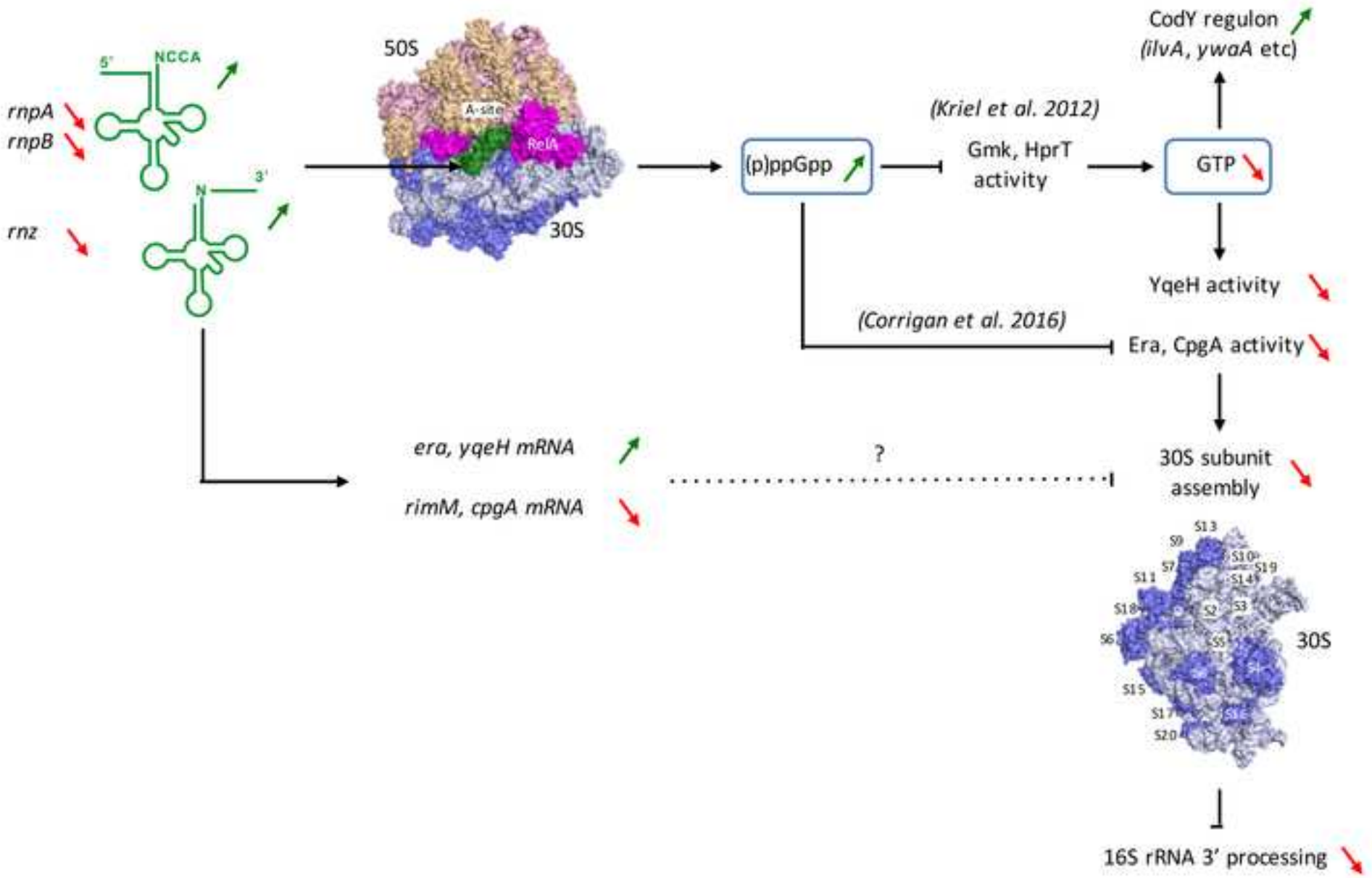

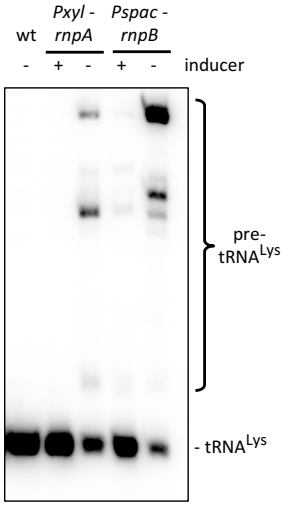

Figure S1, related to Figure 1: Effects of *rnpA* and *rnpB* depletion on processing of $tRNA^{Lys}$. The Northern blot was probed with oligo CC1915, complementary to the mature portion of the *trnJ-lys* tRNA.

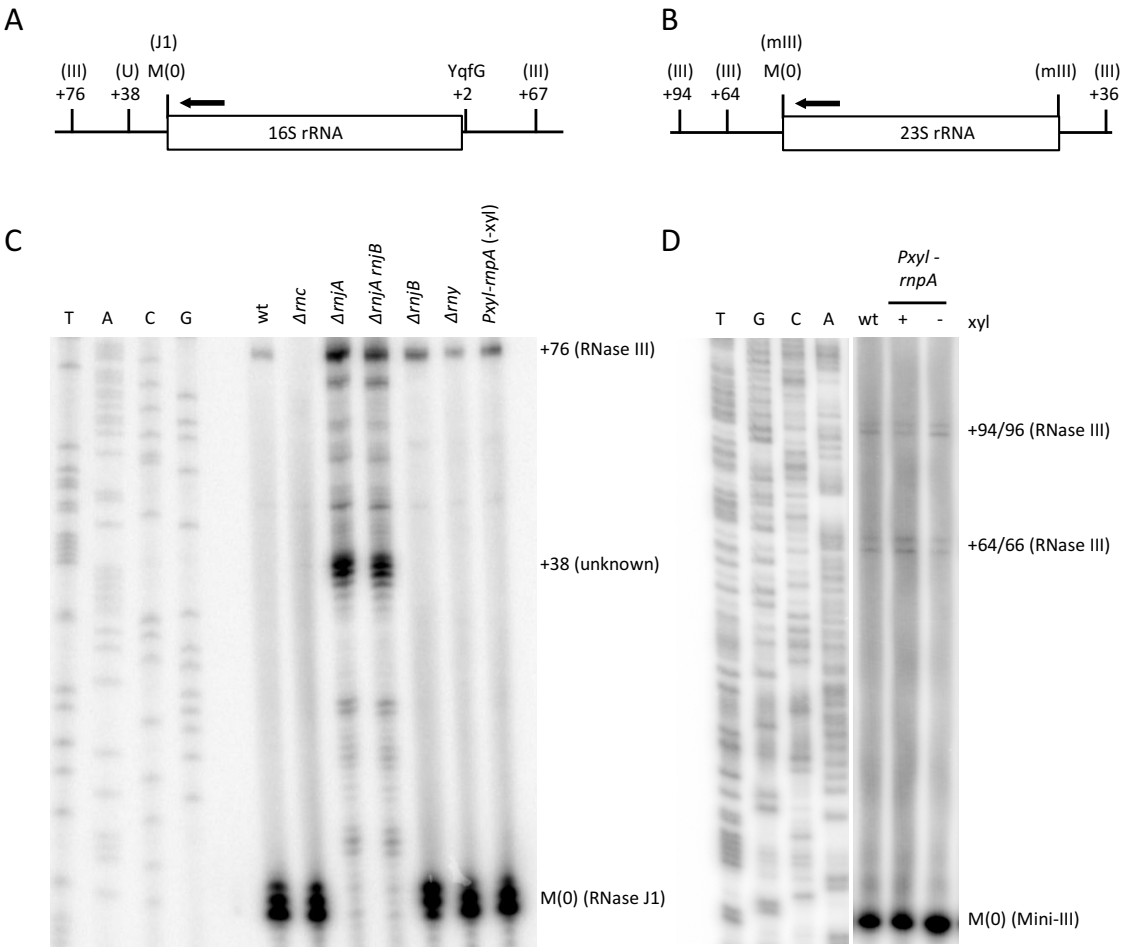

Figure S2, related to Figure 1: RNase P depletion is specific to the 3' processing of 16S rRNA. (A) Schematic of primer extension assay of 16S rRNA 5' processing, showing cleavage sites for RNase III (III), the unknown RNase (U), RNase J1 (J1) and YqfG. The primer used (CC058) is schematized by a black arrow. (B) Schematic of primer extension assay of 23S rRNA 5' processing, showing cleavage sites for RNase III (III) and Mini-III (mIII). The primer used (CC257) is schematized by a black arrow. (C) Primer extension assay of 16S rRNA 5' processing using oligo CC058 performed on total RNA isolated from wild-type (WT) or strains lacking RNase III (Δ*rnc*), RNase J1 (Δ*rnjA*), RNase J2 (Δ*rnjB*), RNase Y (Δ*rny*), or depleted for the protein subunit of RNase P (*rnpA*). (D) Primer extension assay of 23S rRNA 5' processing using oligo CC257, performed on total RNA isolated from WT and the *rnpA*-depletion strain in the absence of xylose (xyl).

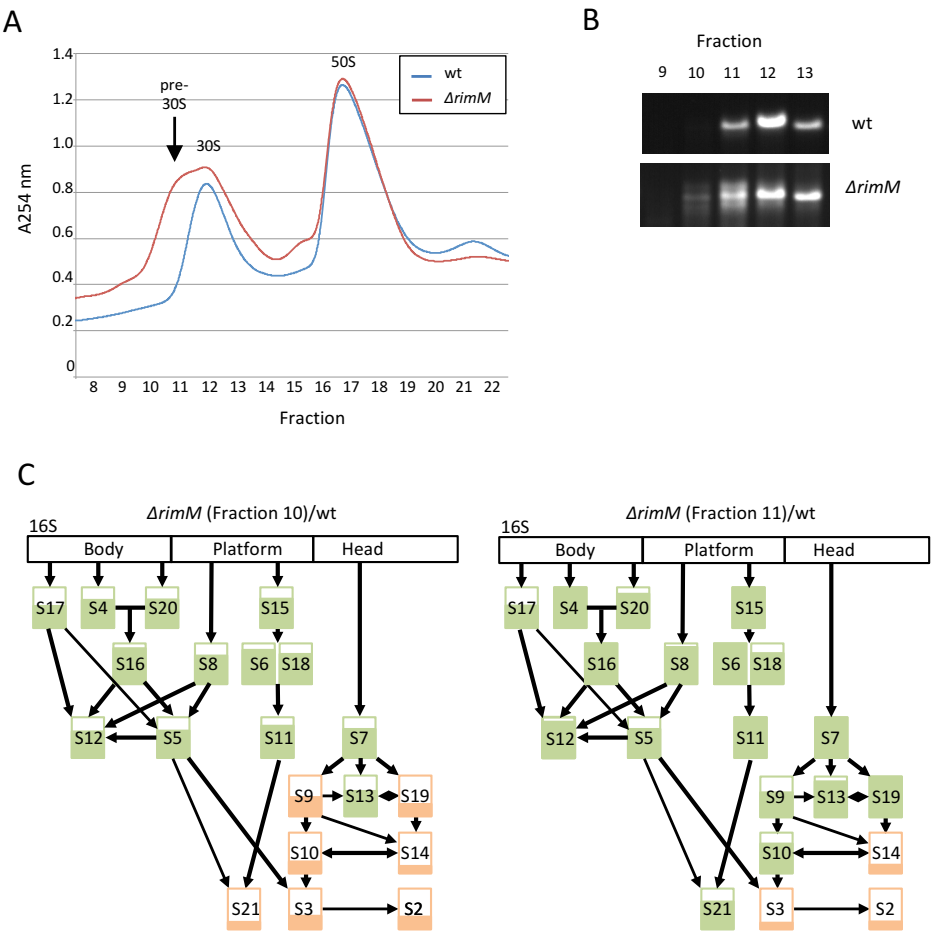

Figure S3, related to Figure 3: The effect of RNase P and Z depletions on ribosome assembly is similar to that of cells lacking the late assembly factor RimM. (A) Sucrose gradients of wt vs *ΔrimM* mutants (B) 16S rRNA profile in sucrose gradients (C) LC-MS/MS analysis (n=2) of pre-30S fractions in wt vs *ΔrimM* mutants. The number of peptides for each protein were first normalized to the total peptides observed in each fraction and then normalized to the equivalent number in wt. Early fraction 10 in the *ΔrimM* mutant was compared to early fraction 11 in wt; late fraction 11 in the *ΔrimM* mutant was compared to mature fraction 12 in wt. The percent fill of each box represents the amount of each ribosomal protein compared to wt. Proteins shown in orange are represented at >10% but ≤ 50% of wt; green > 50% of wt.

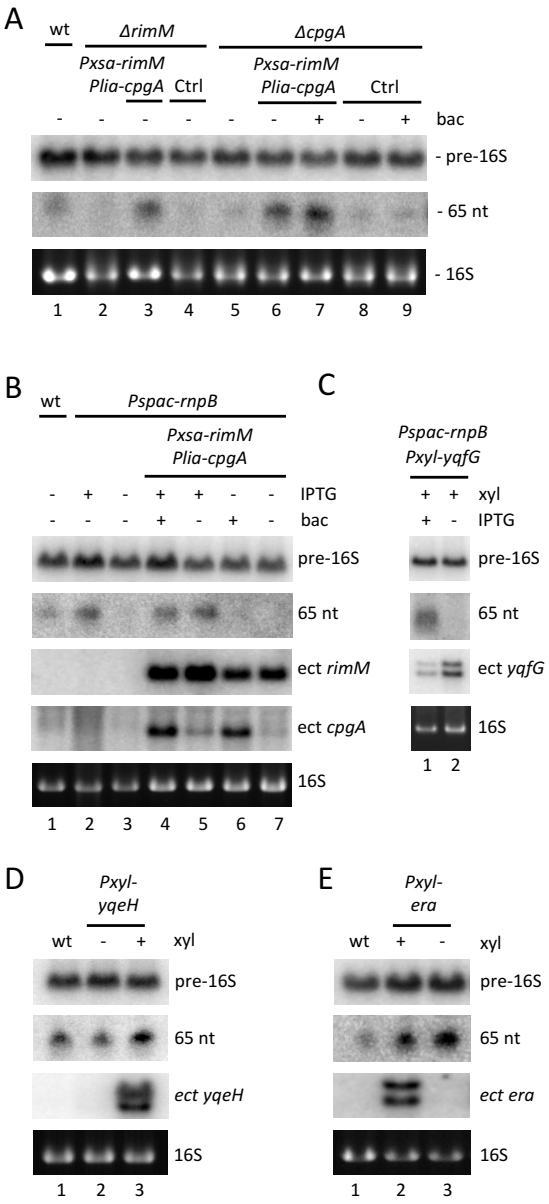

Figure S4, related to Figure 2: Perturbation of individual assembly factor mRNA levels is unlikely to explain defects in 16S 3' processing. (A) The *Pxsa-rimM + Plia-cpgA* vector is functional. Control experiment showing complementation of 16S rRNA 3' processing defects of *ΔrimM* and *ΔcpgA* strains by ectopic expression of *rimM* and *cpgA,* respectively. Note that expression of *Pxsa-rimM* is leaky and yields about 2-fold excess of *rimM* mRNA in the absence of arabinose, compared to expression from the native locus (not shown). Expression of *Plia-cpgA* is also leaky; addition of bacitracin (bac) yields similar levels of *cpgA* mRNA to expression from the native locus (not shown). Ctrl is the empty vector control. (B) 16S 3' processing is not restored in *rnpA*-depleted cells ectopically expressing *rimM* alone or together with *cpgA*. (C) 16S 3' processing is not restored in *rnpA*-depleted cells ectopically expressing *yqfG.* (D)+(E) 16S 3' processing is not inhibited upon over-expression of either *era* or *yqeH* in a wt background. 5 μg of total RNA was probed with oligo CC172, specific for the 16S rRNA 3' precursor, on agarose gels (upper panel) and polyacrylamide gels (lower panel) in each case for optimal transfer of the ~ 1620 nt and 65 nt species.

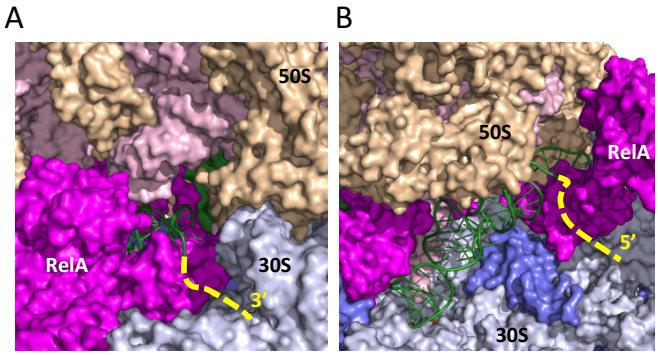

Figure S5, related to Figure 7: RelA bound to the A-site of the ribosome can accomodate tRNA precursors. (A) Possible pathway for tRNA 3' extensions (yellow dotted line). RelA is shown in space filling mode in pink, the 30S subunit in light blue (16S rRNA) and dark blue (30S proteins), the 50S subunit in pink (23S rRNA) and wheat (50S proteins), the A-site tRNA in cartoon mode and the P-site tRNA in space filling mode are shown in green (B) Possible pathway for tRNA 5' extensions. Color scheme as in panel (A).